PHYSICAL REVIEW D **80,** 065031 (2009)

Nonperturbative volume reduction of large-N QCD with adjoint fermions

Barak Bringoltz and Stephen R. Sharpe

Department of Physics, University of Washington, Seattle, Washington 98195-1560, USA

(Received 26 June 2009; published 28 September 2009)

We use nonperturbative lattice techniques to study the volume-reduced ''Eguchi-Kawai'' version of four-dimensional large-N QCD with a single adjoint Dirac fermion. We explore the phase diagram of this single-site theory in the space of quark mass and gauge coupling using Wilson fermions for a number of colors in the range $8 \leq N \leq 15$. Our evidence suggests that these values of N are large enough to determine the nature of the phase diagram for $N \to \infty$. We identify the region in the parameter space where the $(Z_N)^4$ center symmetry is intact. According to previous theoretical work using the orbifolding paradigm, and assuming that translation invariance is not spontaneously broken in the infinite-volume theory, in this region volume reduction holds: the single-site and infinite-volume theories become equivalent when $N \to \infty$. We find strong evidence that this region includes both light and heavy quarks (with masses that are at the cutoff scale), and our results are consistent with this region extending toward the continuum limit. We also compare the action density and the eigenvalue density of the overlap Dirac operator in the fundamental representation with those obtained in large-N pure-gauge theory.

DOI: 10.1103/PhysRevD.80.065031 PACS numbers: 11.15.−q, 11.15.Ha, 11.15.Pg, 12.38.Gc

I. INTRODUCTION

The $1/N$ expansion of $SU(N)$ gauge theories is a particularly useful tool for exploring the nonperturbative dynamics of QCD and related theories. Applications can be found in many areas of research, including the dynamics of confinement, issues related to the phase diagram of QCD, and the relation of QCD to a possible string construction. While large-N methods offer a route to approach certain QCD-related theories with some analytic control, the large-N limit of QCD itself remains unsolved. This makes lattice studies of this limit quite useful, and indeed these have provided a substantial body of nonperturbative information about large-N QCD. This information plays an important role in guiding and testing the approximate analytic approaches to large-N QCD.[1]

One way to approach the large-N limit on the lattice is to use a straightforward generalization of the methods used to simulate QCD. The continuum and infinite-volume limits are taken for various values of N, and the resulting physical quantities then extrapolated to the large-N limit (typical values of N used are $2 \leq N \leq 8$, but in some instances larger values, $N = 10$–16, have been used).

In this paper we use a complementary approach commonly referred to as ''large-N volume reduction.'' The original idea was proposed for lattice regulated theories in the seminal paper by Eguchi and Kawai [2]. One considers a ''latticelike'' matrix model that, under certain assumptions, can be shown to be equivalent to a corresponding (infinite-volume) lattice gauge theory if $N \to \infty$ in both theories. By latticelike we mean a model whose degrees of freedom take values in the group, rather than in its algebra, and that depends on dimensionless couplings and bare masses. The equivalent lattice gauge theory has the same values for these dimensionless couplings and masses. The equivalence is thus to a theory with a fixed cutoff, and one must take the large-N limit before tuning parameters to take the continuum limit.

The idea of Eguchi and Kawai has spawned much interesting work demonstrating large-N equivalences between different theories. The two equivalences that motivate our present work are the orientifold and orbifold equivalences of Refs. [3–5]. Combining these leads to the following result [6].

The large-N limit of infinite-volume lattice QCD with $2N_f$ Dirac fermions in the antisymmetric representation is equivalent, for some observables, to the large-N limit of QCD with N_f Dirac fermions in the adjoint representation defined on a lattice with a finite number of sites N_s. The boundary conditions in all directions for both fermions and gauge fields must be periodic. This equivalence holds, in particular, for the ''single-site theory'' in which $N_s = 1$.

Thus, by studying the large-N limit of the single-site theory with adjoint fermions, we can explore large-N QCD with fermions in the antisymmetric representation. The latter theory has considerable phenomenological interest because it reduces to physical QCD with $2N_f$ fermions in the fundamental representation when $N = 3$. Thus, using the equivalence above, we are able to study a large-N limit of QCD that differs from the standard 't Hooft limit. This alternate limit has the distinguishing feature that fermion loops are present at leading order in the large-N expansion.

In order for the combined equivalence to hold several conditions must be fulfilled [6,7]:

(1) The ground state of infinite-volume large-N QCD with N_f Dirac fermions in the adjoint representation must be translation invariant.

[1]References to the lattice studies can be found, for example, in Ref. [1].

(2) The ground state of infinite-volume large-N QCD with $2N_f$ Dirac fermions in the antisymmetric representation must be charge-conjugation invariant.
(3) The ground state of the large-N single-site QCD with N_f Dirac fermions in the adjoint representations must be $(Z_N)^4$ invariant. This symmetry is the familiar center symmetry in which each of the four Polyakov loops that wind around the four Euclidean compactified directions is independently multiplied by a Z_N factor. (Note that in the single-site model each Polyakov loop is composed of a single link matrix.)

It is also necessary that all theories obey cluster decomposition; the ground state must not be linear combination of vacua that become disjoint at large N. This then implies that multitrace expectation values factorize at large-N. We do not expect cluster decomposition to fail, but we mention this condition for completeness.

Clearly, a crucial question is whether the three conditions listed above actually hold. We have no reason to suspect that the first two conditions fail, and we assume here that they hold. The status of the third condition is less clear. In the following we give a brief summary of relevant results in the literature, from which we conclude that, while there are some reasons to think that the condition holds, what is needed is a direct study of this issue.

First we note that the third condition fails when the quark masses go to infinity. In that limit the single-site theory becomes the Eguchi-Kawai (EK) model, for which analytical and numerical results show that the center symmetry is spontaneously broken at weak coupling [8–10]. This is not necessarily a concern, however, because we are interested in small quark masses, and there are reasons to think that there will be a transition to a phase with restored center symmetry as the quark mass is lowered. In particular, in the limit of zero quark mass, an analysis of the continuum theory on $R^3 \times S^1$, using weak-coupling techniques that are valid when the radius of the S^1 is small enough, finds that the center symmetry (here just Z_N) is unbroken for small radius [6]. The situation at nonzero quark mass has been discussed in Refs. [11]. It appears to us that the conclusion from the last of these papers is that the center symmetry is broken for any nonzero mass when $N \to \infty$. We also note in passing that, for very heavy quark masses, the effect of the fermions is to induce extra interactions between Polyakov loops wrapping around the compactified direction, and from this point of view, the emergent model is in the class of ''deformed EK models'' suggested in Ref. [12], for which the center symmetry is unbroken at weak coupling for a judicious choice of its parameters (for a related study see Ref. [13]).

Very recently, the calculation in Ref. [6] was extended in Ref. [14] to lattice regularization using Wilson fermions. The results were promising: the Z_N symmetric vacuum was seen to have a lower energy than that of the vacua breaking $Z_N \to \emptyset$, for a range of lattice parameters that are physically relevant and that include the chiral point. The results of Ref. [14] also suggest that the center symmetry may be intact even for quite heavy fermions, thus opening a path to study the pure-gauge theory on a lattice with one direction reduced to a point. We note, however, a caveat concerning the results of Ref. [14]: the possibility of more elaborate center-symmetry breaking to nontrivial subgroups of Z_N was not considered. Such symmetry breaking has been found in a different, though similar, setup, in which one uses a continuum regulator in the R^3 directions and a lattice regulator in the S^1 direction [15]. In fact, in this setup the symmetry is found to break even at zero mass.

For completeness, we note that other approaches to large-N reduction have been followed in the literature. Most closely related to the present work is the study of EK reduction in the matrix model obtained by dimensional reduction of $SU(N)$ supersymmetric Yang-Mills theory (the $N_f = 1/2$ case discussed below) [16]. This work differs, however, in using a noncompact representation of the gauge fields. Nevertheless, the evidence found in Ref. [16] that reduction holds for a range of scales is encouraging. See also the related work in Ref. [17].

In addition, for QCD with quarks in the fundamental representation, whose dynamics in the $N \to \infty$ limit are those of the pure-gauge theory, it has been found that volume independence does hold as long as one does not reduce the length of the box below a fixed physical size of $O(1\text{ fm})$ [18] (see also Ref. [19]). Other approaches to repair the center-symmetry breaking problem of the EK model, such as the twisted [20] and quenched [8,9] EK models, have been found recently to fail for weak coupling [21–24].

As can be seen, there are no results that directly address our third condition for the single-site model. In principle, one could extend the perturbative calculation of Ref. [14] to the case where all Euclidean directions are reduced to a point, but this would require dealing with infrared divergences that arise in the single-site theory. In fact, even if such a weak-coupling calculation were done, it would not tell us the center-symmetry realization for moderate couplings, where actual lattice calculations are done. For example, we might find that a weak-coupling calculation points to a Z_N broken phase, but that the larger fluctuations in the gauge fields, which occur as the coupling increases, restore the symmetry. Alternatively, if a one-loop calculation tells us the symmetry is intact, then a sufficiently intricate vacuum manifold could lead to symmetry breaking at strong enough coupling. These possibilities are not just academic exercises as both were observed in related models—for example see the phase diagram of the model studied in Ref. [22].

From the discussion above it is clear that a nonperturbative lattice Monte-Carlo analysis of the single-site model is

required, and this is what we perform in this paper. In particular we focus here on the theory with $N_f = 1$, which is connected, through the equivalences mentioned above, to physical QCD with two flavors. Our results suggest that the $(Z_N)^4$ symmetry is intact for a broad range of quark masses including zero. Thus we are studying a theory which is "within $1/N$" of the infinite-volume theories appearing in conditions (1)–(2) above: QCD at large N with one Dirac fermion in the adjoint representation, QCD at large N with two Dirac fermions in the antisymmetric representation, and, last but not least, QCD at $N = 3$ with two degenerate flavors in the fundamental.

It would also be of considerable interest to study whether reduction holds for other values of N_f. For $N_f = 1/2$, the equivalence is, in the massless limit, to the large-N limit of $\mathcal{N} = 1$ SUSY (and to QCD with a single Dirac flavor). For two colors this SUSY theory was studied on the lattice by various authors [25,26] (see also the review in Ref. [27] and the work noted above on the reduced model in the noncompact theory [16]). The $N_f = 2$ case is of interest as a potential example of a nearly-conformal or conformal theory. Again, for a small number of colors, these theories have been studied on the lattice [28,29].

The following is the outline of the paper. In Sec. II we discuss QCD with N_f adjoint fermions—the theory that our single-site model is potentially equivalent to. We define the theory and describe a conjecture for its phase diagram. In Sec. III, we discuss the corresponding volume-reduced single-site theory—again defining this theory and presenting a conjecture for its phase diagram. Section IV provides some technical details of our lattice Monte-Carlo simulations of the single-site theory. In Sec. V we define the observables we measure and use them to map the parameter space of our model, looking for regimes in which the center symmetry is intact. Section VI includes a restricted set of results of physical interest, such as certain eigenvalue densities of Dirac operators. We summarize our study in Sec. VII and discuss possible future directions of study.

II. LATTICE QCD WITH ADJOINT FERMIONS

If reduction holds, the single-site matrix model discussed in the next section is equivalent, at large N, to lattice QCD with fermions in the adjoint representation in (arbitrarily) large volumes. Here we discuss the properties of the latter theory, so that we know what we should expect to find in the single-site model if reduction holds.

The orbifold construction that underlies this potential equivalence implies that the form of the lattice actions is the same in both the reduced and unreduced theories. We use the Wilson gauge action and Wilson fermions for the matrix model, and so discuss below the same action for the large-volume theory. We thus consider a gauge theory in four Euclidean dimensions, with lattice spacing a and L^4 sites, and whose path integral

$$Z_{\rm adj} = \int DUD\psi D\bar{\psi}\, \exp(S_{\rm gauge} + \bar{\psi} D_W \psi). \tag{2.1}$$

The gauge action is

$$S_{\rm gauge} = 2Nb \sum_P {\rm Re\,Tr} U_P, \tag{2.2}$$

where P labels plaquettes, U_P is product of $SU(N)$ link variables around the plaquette, and b is the inverse 't Hooft coupling that is kept fixed as N is increased

$$b \equiv (g^2 N)^{-1}. \tag{2.3}$$

The N_f Dirac fields ψ carry implicit spatial, spinor, and adjoint color indices. We use the lattice Wilson-Dirac operator

$$(D_W)_{xy} = \delta_{xy} - \kappa \Big[\sum_{\mu=1}^{4} (1-\gamma_\mu) U^G_{x,\mu} \delta_{y,x+\mu} + (1+\gamma_\mu) U^{\dagger G}_{x,\mu} \delta_{y,x-\mu} \Big], \tag{2.4}$$

where x and y label sites, and κ is the usual hopping parameter, related to the bare quark mass by

$$\kappa = \frac{1}{8 + 2am_0}. \tag{2.5}$$

The boundary conditions on both gauge and fermion fields are taken to be periodic.

In a literal implementation, $U^G_{x,\mu}$ would be the adjoint representatives of the $SU(N)$ matrices $U_{x,\mu}$ appearing in the gauge action. Thus U^G would be a matrix of dimension (N^2-1), and ψ an (N^2-1)-dimensional color vector. We find it simpler to place the fermions in the reducible $N \otimes \bar{N} = {\rm adj} \oplus \mathbf{1}$ representation, so that they have N^2 color components, and are acted on by $N^2 \times N^2$ matrices. As will be seen shortly, the additional singlet component decouples from the dynamics.

We denote fundamental representation color indices by lower-case letters, e.g. $a, b \in [1, N]$, and $N \otimes \bar{N}$ indices by upper-case letters, e.g. $A, B \in [1, N^2]$. We choose a basis in which the latter index is composite:

$$A \equiv (a_1; a_2), \tag{2.6}$$

and, correspondingly, in which

$$U^G_{AB} \equiv U^G_{(a_1;a_2),(b_1;b_2)} = U_{a_1,b_1} U^\star_{a_2,b_2}. \tag{2.7}$$

This acts on a fermion field with indices $\psi_B = \psi_{(b_1;b_2)}$. By a change of basis we can bring U^G into block diagonal form, with a 1-d block for the singlet, and an $(N^2-1)-d$ block for the desired adjoint part. The singlet part is, however, unity for all $U \in SU(N)$. This implies that

$${\rm det} D_W(U_{N\otimes\bar{N}}) = {\rm det} D_W(U_{\rm adj}) \times {\rm constant}, \tag{2.8}$$

showing that we obtain the path integral of the desired adjoint theory up to an irrelevant overall constant. To

calculate fermionic expectation values one would, however, need to remove the singlet component.

At tree level in perturbation theory, the quarks become massless when $\kappa = 1/8$, a result which holds for any representation. At higher order, and nonperturbatively, am_0 is additively renormalized, and the true chiral point occurs at $\kappa_c > 1/8$. This is because Wilson fermions break chiral symmetry explicitly for any nonzero lattice spacing. The physical mass is then given by

$$m_{\text{phys}} = \frac{Z_m}{a}\left(\frac{1}{2\kappa} - \frac{1}{2\kappa_c}\right), \tag{2.9}$$

with Z_m a multiplicative renormalization factor that depends on the scheme chosen to define the mass. This factor is finite and of $O(1)$ as long as we consider lattice spacings that are not too small, as we do in practice.

QCD with a single adjoint Dirac fermion is asymptotically free (and quite far from the conformal window explored in Refs. [28,29]), and is expected to confine and spontaneously break its chiral-symmetry. Let us first consider the theory with a chirally symmetric regulator. Because the fermion representation is real, its global symmetry group in the chiral limit is $SU(2N_f)$ and not $SU(N_f)_L \times SU(N_f)$ (for example, see Refs. [30,31]). This symmetry is conjectured to break spontaneously to the flavor group $SO(2N_f)$, generating $2N_f^2 + N_f - 1$ Nambu-Goldstone bosons. For $N_f = 1$ we therefore expect two massless modes. The lattice theory, with Wilson fermions, respects only the $SO(2N_f)$ flavor symmetry (which can be most easily seen by rewriting the action using Majorana fermions). Chiral symmetry is restored only in the continuum limit, and requires tuning κ appropriately. We discuss the situation at finite lattice spacing below when we sketch the phase diagram.

The theory also has a $(Z_N)^4$ center symmetry, each factor corresponding to multiplying all the link elements U_{x,μ_0} on a slice of fixed coordinate x_0 in the μ_0 direction by an element of Z_N. Since the fermions are in the adjoint representation, they are neutral under this symmetry. We expect this symmetry to be unbroken for large volumes, as it is in the pure-gauge theory. The key issue is whether it remains unbroken in small volumes. As discussed in the Introduction, analytical arguments in the case of a single short direction indicate that it will remain unbroken at small volumes if the boundary conditions on all fields are periodic. This is in contrast to what happens when the fermions have antiperiodic boundary conditions, when we do expect the center symmetry to be broken when one passes through the finite-temperature deconfinement transition as the physical length of one of the directions is reduced.

A. Phase diagram of adjoint lattice QCD with $N_f = 1$

As far as we know, there have been no lattice studies of gauge theories with $N_f = 1$ adjoint fermions, even for $N = 2$ or 3. There has been extensive work for $N_f = 2$, with $N = 2$ and 3, both for nonzero temperature (see, e.g., Refs. [32,33]) and at zero temperature [28,29]. As discussed in the Introduction, the latter theories are expected to be conformal or nearly conformal, and are not likely to provide useful guidance for the $N_f = 1$ case. There has also been much work on the $N_f = 1/2$, $N = 2$ theory with both Wilson fermions (as reviewed in Ref. [34]; see Ref. [35] for recent progress) and, more recently, Domain-Wall fermions [25,26]. Here, again, the results do not obviously apply to $N_f = 1$ theories, because the target $N_f = 1/2$ theory is, in the chiral limit, supersymmetric.

In fact, it may well be that QCD—physical QCD with fermions in the fundamental-representation—is the theory whose dynamics is most similar to that of the $N_f = 1$ adjoint theory. Assuming so, we make the educated guess for the phase diagram shown in Fig. 1. Although we are particularly interested in the large-N limit, we expect this sketch to hold also for small values of N.

Let us explain the features of this diagram. The solid (blue) line labeled $\kappa_c(b)$, and ending at $(\kappa, b) = (0.125, \infty)$ is the "critical" line (or possibly lines, as discussed below) along which to the fermions attain their minimal mass. The continuum limit, in which there are light fermions, is obtained by approaching the end point of this line (in a way which depends upon the desired fermion masses).

Close enough to the continuum limit (i.e. for large enough b), the theory in the vicinity of the critical line can be analyzed using chiral perturbation theory including lattice artifacts [36]. The analysis is similar to that for QCD, but must be generalized to the $SU(2) \to SO(2)$

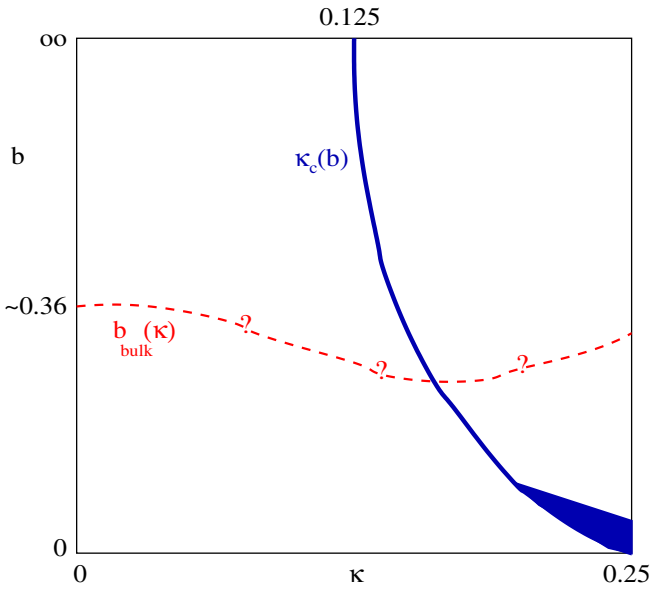

FIG. 1 (color online). Conjectured phase diagram in the $\kappa - b$ plane for a QCD-like theory with a single Dirac adjoint fermion. Details are discussed in the text.

chiral-symmetry-breaking pattern. In fact, the corresponding case for $N_f = 2$ adjoints $[SU(4) \to SO(4)]$ has been worked out in Ref. [37], and the generalization to our case is straightforward. One finds that, as in QCD, there are two possibilities: either there is a line of first-order transitions, at which the two degenerate pseudo-Goldstone "pions" attain their minimal (nonzero) mass, or there are two lines of second-order transitions, at which the masses of both pions vanish. Between these second-order lines lies an Aoki phase [38], in which the $SO(2)$ flavor symmetry of the lattice theory is spontaneously broken, so that one of the pions is exactly massless, while the other is massive. As $b \to \infty$, the nonzero pion masses in both scenarios go to zero linearly with a. In addition, the width of the Aoki phase, if present, shrinks as a^3.

One cannot predict which scenario applies without a nonperturbative calculation, and the result depends on the details of the action. The numerical results discussed below suggest that the transition is first order (and thus that κ_c is a single line) for $b \gtrsim 0.1$ (which is the smallest value we use). It is worth stressing that, in either scenario, one can approach the continuum limit on either side of the transition(s), i.e. with $\kappa < \kappa_c(\text{min})$ or $\kappa > \kappa_c(\text{max})$. The two sides have identical long-distance physics as $a \to 0$.

As one moves to stronger coupling, terms of higher order in a become important, and it is possible that one changes from a first-order transition to having an Aoki phase, or more exotic possibilities. Once at very strong coupling, $g^2 N \gg 1$, one can show that there will be an Aoki phase, and that $\kappa_c \to 1/4$ when $b \to 0$. This is because the analysis of lattice QCD in this limit carried out in Ref. [39] holds also for the theory with fermions in the adjoint representation.[2] Because of this, we have shown a region (solid [blue] shading) of Aoki phase for $b \lesssim 0.1$.

For $\kappa \geq \frac{1}{4}$ there will be additional phase structure (the Aoki phase "fingers"), with additional critical lines along which the continuum theory has more than one light Dirac fermion (four or six, depending along which critical line one takes the continuum). These continuum theories are not asymptotically free, and are not interesting for our purposes of connecting to physical QCD. Thus we have restricted our attention to $\kappa < \frac{1}{4}$.

The other feature shown in Fig. 1 is the approximately horizontal (red) dashed line punctuated with question marks. This indicates a possible "bulk" transition, so we label it $b_{\text{bulk}}(\kappa)$. For $N \geq 5$ such a transition is known to be present at $\kappa = 0$ (i.e. the pure-gauge theory) and to be strongly first order (for lower values of N it is a crossover). We therefore expect that it persists as a first-order transition line for some distance out into the $\kappa - b$ plane. We emphasize that this transition is a lattice artifact and so the bare coupling at which it takes place approaches a nonzero (and noninfinite) κ-dependent value for infinite volume and infinite N. For example, it occurs for $\kappa = 0$ at $b_{\text{bulk}}(\kappa = 0) \simeq 0.36$ as indicated in the Figure.[3] This transition is also not associated with any symmetry breaking and so can end anywhere in the $(\kappa - b)$ plane. In the absence of any data we do not know what happens and so decorate the dashed line by question marks. In any event, since the continuum limit is at $b = \infty$, lattice simulations aiming to approach that limit should be made for $b > b_{\text{bulk}}(\kappa)$.

III. THE VOLUME-REDUCED THEORY AND ITS PHASE DIAGRAM

We now turn to the single-site theory which is the focus of the present work. It is defined simply as the $L = 1$ version of the construction in Eq. (2.1), and is the generalization of the original EK model obtained by adding adjoint fermions. The degrees of freedom in the model are the four $SU(N)$ matrices $U_{\mu=1-4}$, and the $4N^2$-component Grassmann variables ψ and $\bar{\psi}$. The action of this adjoint EK (AEK) model is

$$S_{\text{AEK}} = S_{\text{EK}} + \bar{\psi} D_W^{\text{red}} \psi, \tag{3.1}$$

$$S_{\text{AEK}} = 2Nb \sum_{\mu<\nu} \text{Re Tr} U_\mu U_\nu U_\mu^\dagger U_\nu^\dagger, \tag{3.2}$$

$$D_W^{\text{red}} = 1 - \kappa \sum_{\mu=1}^{4} [(1 - \gamma_\mu) U_\mu^G + (1 + \gamma_\mu) U_\mu^{\dagger G}]. \tag{3.3}$$

For the purpose of Monte-Carlo simulations, we formally integrate over the fermions and evaluate expectation values with the following path integral:

$$Z_{\text{AEK}} = \int_{SU(N)} \prod_{\mu=1}^{4} DU_\mu \exp[S_{\text{EK}} + \log \det(D_W^{\text{red}})]. \tag{3.4}$$

[2]This holds despite the fact that the symmetry-breaking pattern is different. For example, one of the pions which becomes massless is created by the "diquark" operator $\psi^T C \gamma_5 \psi$. For $g^2 N \gg 1$, the propagator for this diquark has, in a hopping-parameter expansion, both quarks hopping along the same path, so that gauge matrices completely cancel from the "pion" propagator, just as for quark-antiquark pair in QCD in this limit. One can furthermore show that the Dirac-matrix factors are the same in the two calculations. Thus the propagators in the two theories are proportional, and so the corresponding pion masses vanish at the same κ.

[3]The value of $b_{\text{bulk}}(\kappa = 0)$ was measured, for example, by hysteresis scans [40]. A result is also given in Ref. [41], but using the simulations of the "twisted EK" model, a variation of the EK model that was recently invalidated for large enough values of N [22,23]. Nonetheless, it is possible that reduction holds for the values $N \leq 64$ used in Ref. [41], and that the estimate for $b_{\text{bulk}}(\kappa = 0)$ obtained there is reliable.

The relevant symmetries of $Z_{\rm AEK}$ are the same as those of the original EK model. They are the remnant of the gauge symmetry

$$\forall\ \mu\colon U_\mu \to \Omega U_\mu \Omega^\dagger \quad \text{with} \quad \Omega \in SU(N), \tag{3.5}$$

as well as center transformations applied independently to the four link matrices

$$U_\mu \to U_\mu z^{n_\mu} \quad \text{with} \quad z = e^{2\pi i/N} \quad \text{and} \quad n_\mu \in Z_N. \tag{3.6}$$

As explained in Sec. I, large-N equivalence holds as long as the $(Z_N)^4$ symmetry in Eq. (3.6) is unbroken. We recall here how this equivalence works in detail. This equivalence states that appropriate expectation values in the reduced theory become identical when $N \to \infty$ to those in the infinite-volume theory defined by Eq. (2.1). Appropriate expectation values in the large-volume theory are the connected correlators of $(Z_N)^4$-invariant and translation-invariant operators. These are mapped into operators in the reduced theory following the prescription of Refs. [2,6]. For example, consider the large-volume expectation value of the plaquette,

$$u \equiv \frac{1}{N}\frac{1}{N_P}\sum_P \langle \mathrm{tr} U_P \rangle_{Z_{\rm adj}}. \tag{3.7}$$

The notation $\langle , \rangle_{Z_{\rm adj}}$ means that we calculate expectation values in the ensemble defined by the partition function in Eq. (2.1). N_P is the number of plaquettes, which in four dimensions is equal to $6L^4$. The corresponding single-site expectation value is

$$u_{\rm red} \equiv \frac{1}{N}\frac{1}{6}\sum_{\mu<\nu} \langle \mathrm{tr} U_\mu U_\nu U_\mu^\dagger U_\nu^\dagger \rangle_{Z_{\rm AEK}} \tag{3.8}$$

so that, in fact,

$$u_{\rm red} = u(L=1). \tag{3.9}$$

The meaning of volume reduction is that

$$u(b,\kappa) = u_{\rm red}(b,\kappa) \tag{3.10}$$

when $N \to \infty$ in both theories.

Our aim in this paper is to find the regions of the $b-\kappa$ plane in which the ground state of the single-site model is invariant under the $(Z_N)^4$ center symmetry, so that equivalences of the form of Eq. (3.10) hold. We first collect what is known about the single-site theory, together with some conjectures, into a phase diagram.

For infinitely massive fermions (i.e. for $\kappa = 0$), our theory becomes the original EK model. This is known to break the $(Z_N)^4$ symmetry for $b > b_{\rm EK} \approx 0.19$ and numerical evidence suggests that the transition is first order [8,10,42]. A crucial issue is then whether, for $b > b_{\rm EK}$, an increase in κ can lead to the restoration of the center symmetry. This is what one would expect based on the results of Refs. [6,14]. Specifically, Ref. [14] studied a lattice theory similar to Eq. (3.1) but in which only one of the Euclidean dimensions is reduced to a point. This weak-coupling calculation found that, for the $N_f = 1$ theory, the center symmetry is broken for $\kappa = 0$, but restored once $\kappa \gtrsim 0.04$. There is, in addition, a small intermediate phase between the two in which the Z_N symmetry is broken down to a Z_2 subgroup. Finally, when κ grows even more, to values above ~ 1.4, the Z_N symmetry is completely broken again.

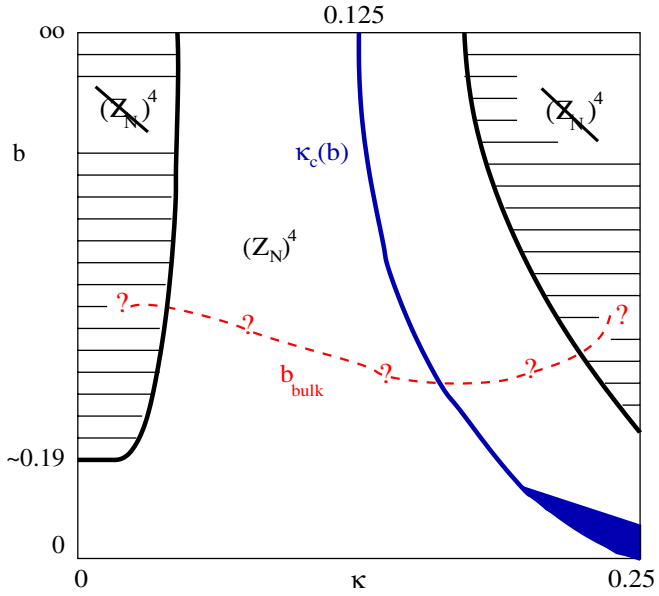

FIG. 2 (color online). Conjectured phase diagram for the single-site model in the large-N limit. Details are discussed in the text.

It is unclear how the fact that in the current paper we study a theory where all lattice directions are reduced to a point changes the results of Ref. [14]. Nevertheless, assuming that the results of Ref. [14] provide a qualitative guide, we are led to conjecture the phase diagram shown in Fig. 2. In the following we describe the features of this diagram.

First, consider the solid (black) line which begins at $b_{\rm EK} \sim 0.19$ on the b axis, bends up, and ends on the top of the diagram. Our conjecture is that this separates a center symmetry-broken phase to the left (shown shaded) from an unbroken phase to the right. This is based on what we know about the EK model, and the assumption that the results of Ref. [14] apply qualitatively to our model. (Note that there can only be a phase transition when $N \to \infty$, while for finite N this will be smoothed out into a crossover.) It is possible that this line actually has a nonzero width and contains intermediate partially broken phases.[4]

[4]For example, this was seen in Ref. [42] at $\kappa = 0$.

We stress that we do not know the value of κ at which this line hits the $b = \infty$ axis, but our conjecture is that this value is smaller than (likely significantly smaller than) $\kappa = 0.125$.

Toward the right-hand side of the plot there is another solid (black) line which also separates the conjectured central center-symmetric phase from a shaded symmetry-broken phase or phases. Here we actually expect a very complicated phase diagram, based on the fact that there are regions where the corresponding infinite-volume theory has multiple light fermions (as discussed above), and the results of Ref. [14]. Since this is not our region of interest, we have not tried to fill in the details. What is important here is the conjecture that this symmetry-broken region lies (significantly) to the right of the critical line (consistent with the results for Ref. [14]).

Given these conjectures, we are left with a central ''funnel'' in which reduction holds, and thus have reproduced both the critical ''line'' $\kappa_c(b)$ and the possible bulk transition line from our conjecture for the infinite-volume theory, Fig. 1. The key question for our numerical investigation is whether this central funnel, and, in particular, its upper part (where one can take the continuum limit) is actually present. We stress again that the precise position of the boundaries of this funnel are supposed to represent only the conjecture that there is a generous region on either side of κ_c in the symmetry-unbroken phase.

Reduction does not hold in the regions where the $(Z_N)^4$ is broken. For this reason we have changed the character of the dashed (red) $b_{\rm bulk}(\kappa)$ line outside of the central funnel. In particular, we are not aware of numerical evidence for a bulk transition for $\kappa = 0$ beyond $b_{\rm EK}$ and did not ourselves observe one. Thus, we end the line away from the b axis. We stress that it is not *a priori* known whether there is a bulk transition at all for any value of κ.

In the next sections we study the theory defined by Eq. (3.4) using nonperturbative Monte-Carlo simulations, and indeed find a phase diagram similar to that appearing in Fig. 2.

IV. NONPERTURBATIVE LATTICE STUDIES: TECHNICAL DETAILS

We study the path integral in Eq. (3.4) using Monte Carlo simulations. The weight function is

$$P(U) = e^{S_{\rm EK}(U)} \det D_W^{\rm red}(U), \tag{4.1}$$

which is integrated using the $SU(N)$ Haar measure for each link: $\prod_{\mu=1}^{4} dU_\mu$. For a single Dirac fermion in the adjoint representation, $\det D_W^{\rm red}$ is real and positive, so that $P(U)$ can be treated as a probability density. The reality of the determinant follows as usual from γ_5 hermiticity $[\gamma_5 D_W^{\rm red} \gamma_5 = (D_W^{\rm red})^\dagger]$. Positivity follows because the fermion is in a real representation, which allows the action to be rewritten in terms of two Majorana fermions, each of which gives a Pfaffian when integrated out. The Pfaffian is real, though of indeterminate sign, but its square is necessarily positive [34].

To produce the field configurations we use a standard Metropolis algorithm. Following Cabibbo and Marinari [43], our proposed changes are obtained by multiplying the links by matrices living in $SU(2)$ subgroups of $SU(N)$. For each subgroup, we propose five changes, and then run through the $N(N-1)/2$ $SU(2)$ subgroups in turn. We repeat this for each of the four links. To calculate the change in $P(U)$ we simply calculate the determinant anew after each suggested change in the links. The $10N(N-1)$ proposed changes just described constitute what we call a ''model update.''We perform measurements every five model updates, after a number of initial ''thermalization'' updates. We found that we could attain acceptance rates of 50–60%.[5]

Since the cost of calculating the determinant of an $M \times M$ matrix scales like M^3, the cost of each of the $SU(2)$ updates scales like N^6, and the overall cost of a model update scales like N^8. This means that, for a fixed number of model updates, a calculation with $N = 15$ is 25 times more expensive than one with $N = 10$. Our resources for this calculation were very modest—roughly an average of four Intel(R) 6700 @ 2.66 GHz CPUs. We did not attempt to parallelize our code, and since we have a single lattice site, it is not clear to us if this is possible. On a single CPU, an $SU(10)$ calculation including 50 thermalization model updates and 100 measurements (550 model updates altogether) took around 3.5 h. We also found that the asymptotic N^8 scaling held to reasonable approximation (so that gathering 500 model updates in $SU(15)$ takes about three days, explaining the modest data set we collected for that gauge group). We note that it may not be necessary to update all the $SU(2)$ subgroups of $SU(N)$ in a single model update—such a procedure is perhaps more suitable for pure-gauge models whose computational scaling law is a moderate N^3. Nevertheless, because our calculation is the first of its kind, we aimed to be conservative and to avoid autocorrelations between successive measurements to the extent possible.

In the following, all errors have been calculated using the jackknife procedure. In some measurements, we varied the bin size and chose a value for which the statistical error saturated. In other measurements, however, we worked with a fixed bin size, and in these cases, based on our

[5]We did so by preparing a list of 800 random $SU(2)$ matrices (and their inverses) such that their traces were Gaussianly distributed around the unit matrix with a width w that decreased with increasing b and N. For example, for $N = 8$, w was ~ 0.5 for $b = 0.1$, ~ 0.05 for $b = 0.30$, and ~ 0.01 for $b = 1.0$. Compared to $SU(8)$, the width w of $SU(15)$, was decreases by about 20%. The distribution in the other, angular, directions in the $SU(2)$ manifold were uniform.

TABLE I. Details of runs that consisted of 100–400 measurements.

Gauge group	b	κ
$SU(8)$	0.35	0.065–0.22
	0.10–0.50	0.001–0.40
	1.00	0.05–0.20
	10^{-5}–1.00	0.03, 0.04
$SU(10)$	0.30	0.01–0.20
	0.35	0.065–0.22
	0.40	0.13–0.18
	0.40	0.13–0.18
	0.50	10^{-3}–0.495
$SU(11)$	0.30	0.03, 0.06
	0.50	0.03–0.33
	1.00	0.09
$SU(13)$	0.50	0.06–0.155
	0.35	0.15–0.20
$SU(15)$	0.50	0.06–0.155
	1.00	0.09

TABLE II. Details of longer runs.

Gauge group	b	κ	Number of configurations
$SU(10)$	0.35	0.1275, 0.150, 0.155	1000
	0.50	0.1275	
	1.00	0.09, 0.1275	
$SU(13)$	1.00	0.09	3700

experience with variable bin sizes, we multiplied the resulting statistical error by a factor of 2. This factor is chosen to be conservative.

We conclude this section by presenting in Tables I and II, the details of the gauge configurations we have accumulated. We typically used 50 model updates for thermalization before starting measurements.

V. NON-PERTURBATIVE LATTICE STUDIES: RESULTS

In this section we present the results of our Monte-Carlo studies and focus on the way the center symmetry is realized in various regions of the phase diagram. The results in Secs. V B, V C, V D, and V E are from the runs in Table I, while those in Sec. V F are from the longer runs in Table II.

A. Definition of observables

The observables we use to map the phase diagram are listed below. They were chosen to probe the large number of possible breaking patterns of the center symmetry (as described, for example, in Ref. [13]), as well as to detect phase transitions that do not involve a change in the realization of the center symmetry.

(1) Plaquette $u_{\rm red}$ as defined in Eq. (3.8).
This observable is not an order parameter for center symmetry, but allows us to detect transitions that are unrelated to the center realization. These include a possible bulk transition at $b_{\rm bulk}(\kappa)$, which would separate the lattice strongly-coupled phase from the continuum one (see Fig. 2), and the $\kappa_c(b)$ line to which one needs to tune to obtain the minimal quark mass.

(2) The expectation values of the traces of four link variables $P_\mu \equiv \frac{1}{N}\,\mathrm{tr}U_\mu$, and their magnitudes $|P_\mu|$. We often refer to these variables as "Polyakov loops."
The P_μ are order parameters for the complete breaking of the center symmetry, though they are not sensitive to partial breaking. The $|P_\mu|$ are probes of large-N factorization: they scale like $1/N$ if factorization holds, but like N^0 if it breaks down.

(3) The expectation values of the traces of the 12 "corner variables" $M_{\mu\nu} \equiv \frac{1}{N}\,\mathrm{tr}U_\mu U_\nu$ and $M_{\mu,-\nu} \equiv \frac{1}{N}\,\mathrm{tr}U_\mu U_\nu^\dagger$ (with $\mu > \nu$), and their magnitudes $|M_{\mu,\pm\nu}|$.
These observables were identified in Ref. [24] as probing a nontrivial form of symmetry breaking characterized by correlations between the link matrices, U_μ, in different directions.

(4) For some parameters we also calculate the following set of $(L+1)^4$ traces:

$$K_{\vec{n}} \equiv \frac{1}{N}\,\mathrm{tr}U_1^{n_1}U_2^{n_2}U_3^{n_3}U_4^{n_4}, \quad \text{with} \quad n_\mu = 0, \pm 1, \pm 2, \ldots, \pm L, \tag{5.1}$$

where $U^{-n} \equiv U^{\dagger n}$. We take $L = 5$ and so calculate 14 641 different averages for each gauge configuration.
Like the $M_{\mu,\pm\nu}$, these traces are order parameters for intricate symmetry breakdown schemes [such as $(Z_N)^4 \to Z_N$ or $(Z_N)^4 \to (Z_N)^3 \times Z_{N/2}$, etc.].

B. Results for $\kappa = 0$: Infinitely heavy quarks

We begin by making a connection with the original EK model (obtained when $\kappa = 0$), for which the behavior is known from previous work. This corresponds to moving up the left-hand axis of Fig. 2. We show in Fig. 3 scatter plots of the four Polyakov loops for three values of b at $N = 10$. The smallest value, $b = 10^{-6}$, is clearly in the strong-coupling regime where, as discussed in Sec. III, we expect the center symmetry to be intact. That this is the case is shown by the clustering of P_μ around the origin. As b increases, the distribution spreads out while remaining centered on the origin (not shown), until one reaches

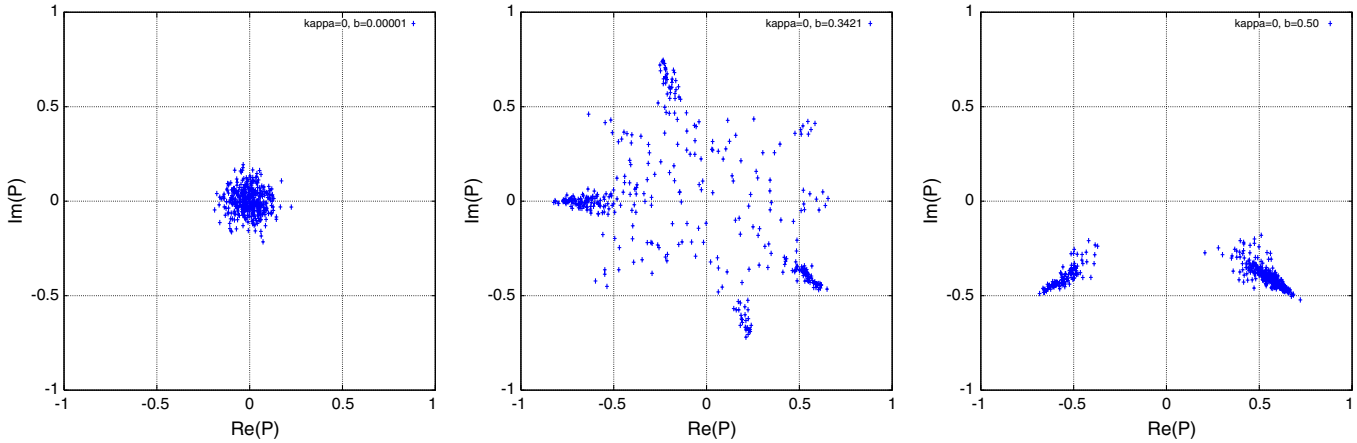

FIG. 3 (color online). Scatter plots of the four Polyakov loops for $N = 10$ and $\kappa = 0$. The values of the coupling are $b = 10^{-6}$ (left), $b = 0.3421$ (middle), and $b = 0.5$ (right).

$b \approx 0.19$, at which point center-symmetry breaking is observed.[6] An illustration of the behavior well inside the symmetry-broken phase is shown in the right two panels, which are for $b = 0.3421$ and 0.5. The Polyakov loops are seen to mainly fluctuate around elements of the center of $SU(10)$, up to an overall scaling factor, i.e. $\langle P_\mu \rangle_{Z_{\mathrm{AEK}}} \sim p_0 e^{2in_\mu \pi/10}$, with $p_0 \approx 0.7$. For $b = 0.3421$ there are also tunneling transitions between different center phases. Although at finite N one does not have a phase transition in the single-site model, these figures show that one can nevertheless observe the putative phase structure even at moderate values of N. Indeed, we obtained similar results (not shown) for $N = 8$.

The nature of the transition is shown in more detail in Fig. 4, which displays the results of a scan in b at $\kappa = 0$ for $N = 10$.[7] There is a rapid rise in the plaquette starting at $b \approx 0.19$, and a corresponding increase in the average magnitude of the Polyakov loop. Note that this "transition" is *not* related to the bulk phase transition of lattice gauge theories, for the latter does not break the center symmetry. We find that, while $N = 10$ is large enough to show a clear indication of the phase transition, it is too small to see a true hysteresis curve (i.e. with a nonzero range of metastability).

C. Results for $\kappa > 0$: Dynamical quarks

We now ask what is the effect of increasing κ from zero, i.e. of decreasing the mass of the adjoint quarks from infinity. Most interesting is to measure this effect for values of b for which the center symmetry is broken at $\kappa = 0$. As an illustration we show in Fig. 5 the scatter of P_μ in the complex plane for a range of κ values at $b = 0.3$ and $N = 10$. We observe that symmetry remains broken at $\kappa = 0.03$, but appears to be restored for $\kappa = 0.06$ and above. That the symmetry is restored at such a small value of κ is consistent with the weak-coupling analysis of Ref. [14]. It is encouraging for our purposes since it indicates that even very heavy adjoint quarks are sufficient to recover the reduction that is absent in the EK model.

We find that the restoration of the center symmetry also holds both for weaker couplings—as in the $b = 0.5$ data

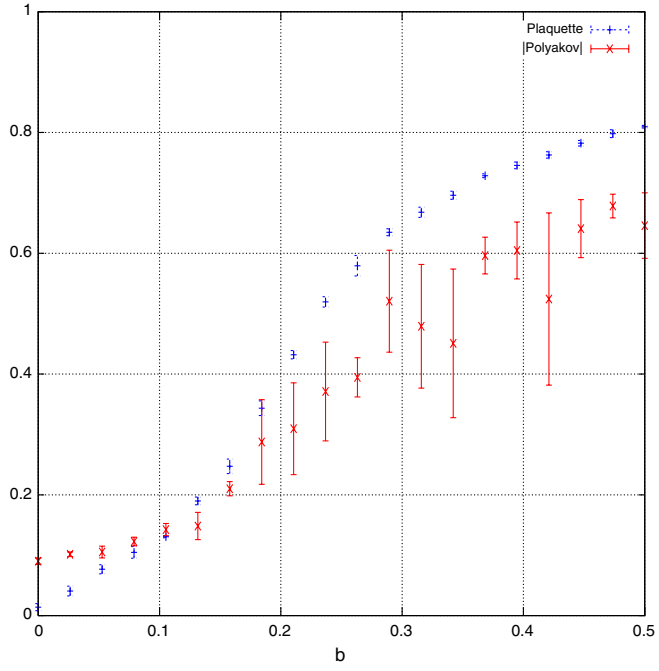

FIG. 4 (color online). Plot of the average plaquette ([blue] pluses) and the magnitude of the Polyakov loop $P_{\mu=1}$ ([red] crosses) at $\kappa = 0$ as a function of b for $N = 10$.

[6] As noted above, this occurs by a cascade of transitions, analogous to those observed in Refs. [42].

[7] In this and subsequent scans, the number of thermalization runs at each value of b was 50, and 100 measurements were performed. The initial gauge configuration for each value of b was the final gauge configuration at the preceding value of b. The first b simulated was that at $b = 0$, where the initial configuration had $U_{\mu=1-4} = 1$.

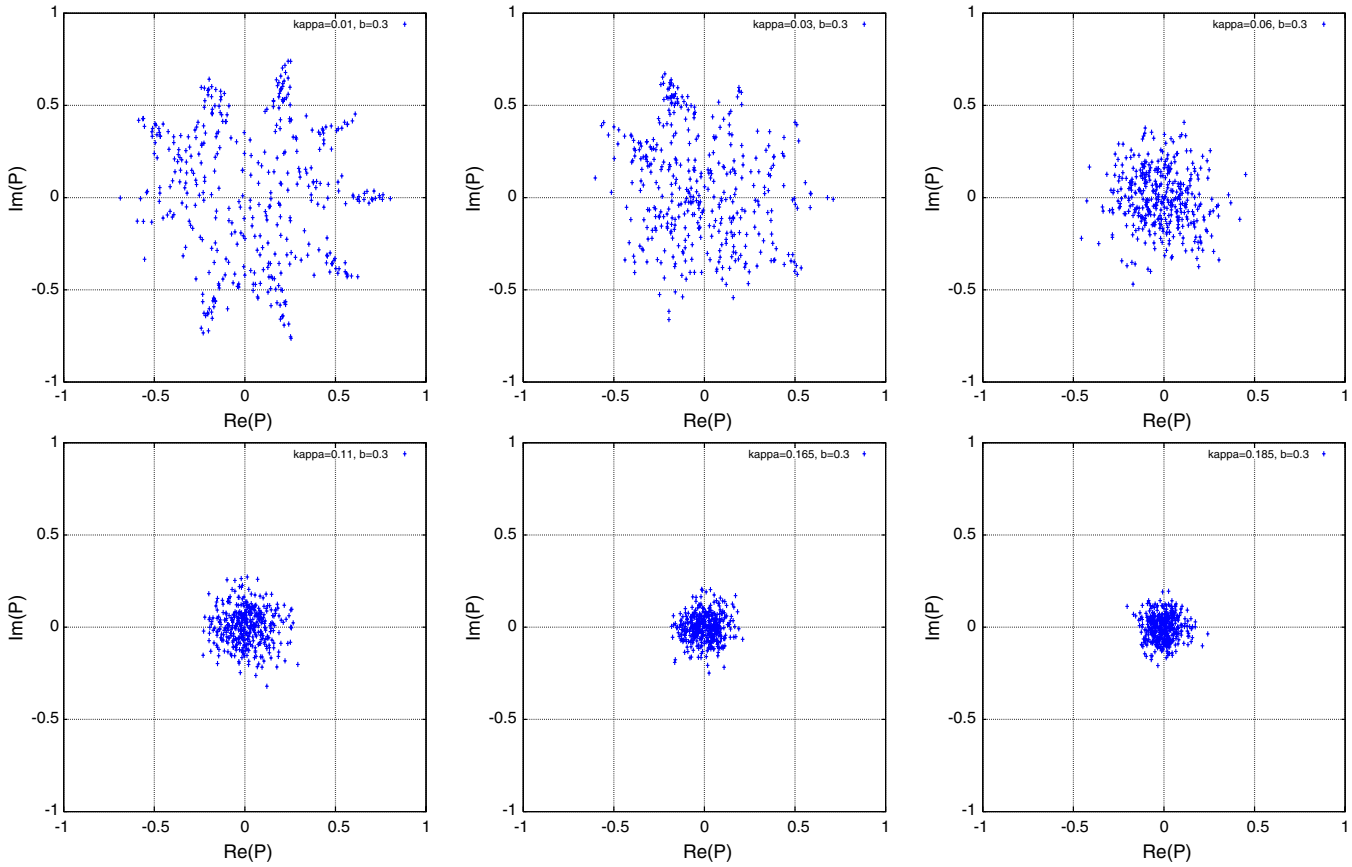

FIG. 5 (color online). Scatter plots of the four Polyakov loops for $b = 0.3$ and $N = 10$. The value of κ increases from the top-left plot to the bottom-right plot in the order 0.01, 0.03, 0.06, 0.11, 0.165, and 0.185.

shown in Fig. 6—and for larger values of N—as exemplified by the $N = 15$, $b = 0.5$ results shown in Fig. 7. (Note that the first nonzero value of κ in the $N = 15$ plots is 0.06 and not 0.03, unlike in the previous plots.) We observe that for $\kappa \geq 0.06$ the fluctuations in the Polyakov loops do decrease as N increases, qualitatively consistent with the expected $1/N$ falloff if one has large-N factorization. Another way to see this is to look at the Monte-Carlo time history of the Polyakov loops. We present examples for $N = 8$, 10, and 15 at $b = 0.5$ in Fig. 8. We observe that the P_μ fluctuate around zero, with an amplitude that decreases as N increases.[8]

So far, our results are consistent with the left-hand part of the conjectured phase diagram of Fig. 2, i.e. with the center-symmetry-broken phase ending for small κ. To investigate further, we have done scans in b for fixed nonzero κ. The left panel of Fig. 9 compares, for $N = 10$, the scan of the plaquette for $\kappa = 0$ (already shown above) to that for $\kappa = 0.0925$ (well into the putative symmetry-restored phase). The right panel shows the corresponding scans for $|P_{\mu=1}|$. We see that the would-be center-breaking transition at $b \approx 0.19$ for $\kappa = 0$ is replaced by a new structure at larger values of $b \simeq 0.28$–0.30, and that this new structure is *not* accompanied by an increase in $|P_1|$. Thus, although there may be a transition for $\kappa = 0.0925$, it is not associated with center-symmetry breaking. It is in fact not clear from our study whether there is such a bulk transition at all. In either case, it is clearly safer to work on the weak-coupling side of this possible transition when trying to make contact with the continuum. This does not, however, appear to pose any difficulty, since our data is consistent with the Z_N symmetry being intact even at $b = 0.5$ (and, less convincingly, at $b = 1.0$ as well—see below).

D. Looking for the chiral point

We now turn our attention to finding the critical line (or lines), $\kappa_c(b)$, that were discussed in Secs. II and III and appear in both Figs. 1 and 2. To do so we performed scans for $0 \lesssim \kappa \lesssim 0.5$ at several values of b and N. We begin by discussing the results of a hysteresis scan (i.e. a scan done by both increasing and decreasing in κ) for $SU(8)$ at $b = 0.35$. The results are presented in Fig. 10. The left panel of the figure shows the plaquette and reveals a very strong

[8]The relatively long decorrelation times evident in these plots suggest that longer runs may be needed for some parameters. We return to this point in Sec. V F.

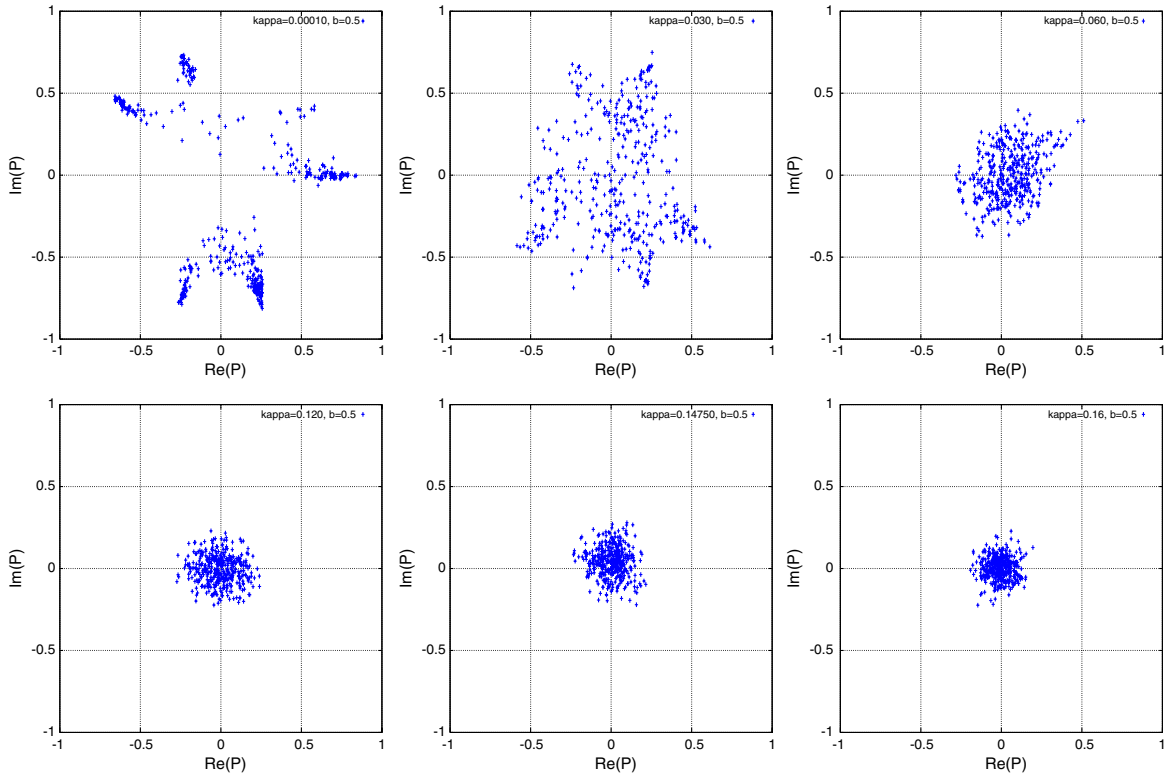

FIG. 6 (color online). As in Fig. 5 but for $b = 0.5$, and for κ values 0.0001, 0.03, 0.06, 0.12, 0.1475, and 0.16 (from top-left to bottom-right).

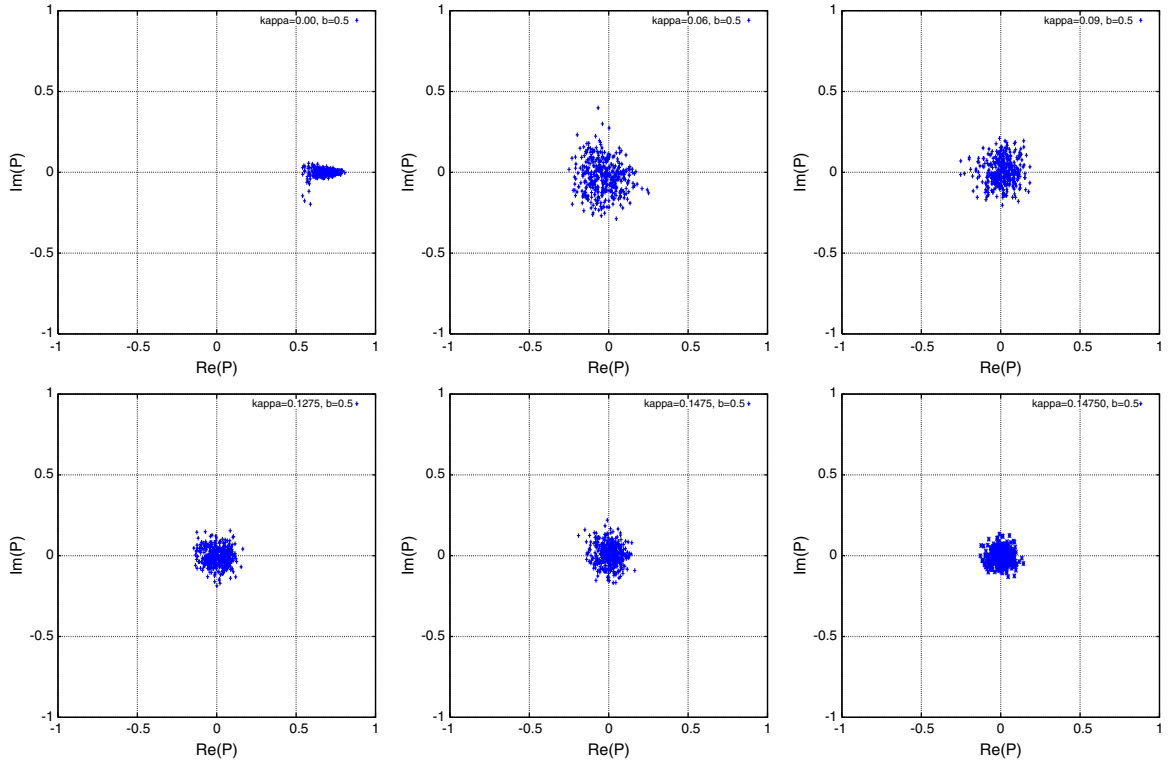

FIG. 7 (color online). As in Fig. 6 but for $N = 15$ at $b = 0.5$. The values of κ are 0, 0.06, 0.09, 0.1275, 0.145, and 0.155 (from top-left to bottom-right).

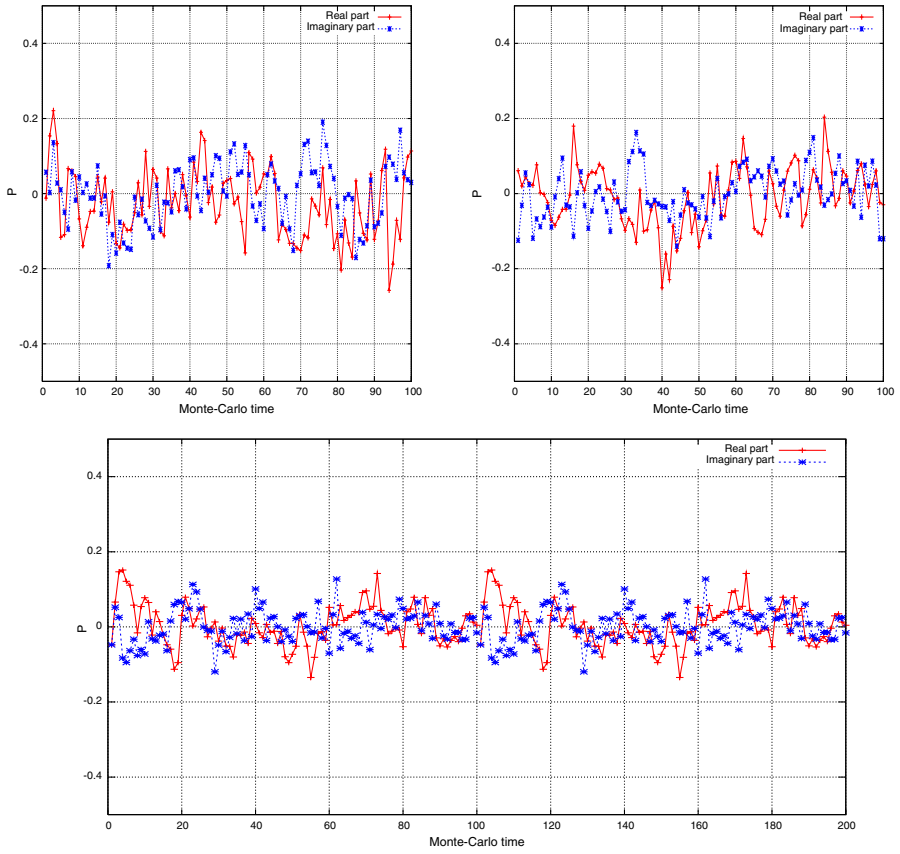

FIG. 8 (color online). Monte-Carlo time history of the Polyakov loop $P_{\mu=1}$ for $N = 8$, 10 (upper panels) and $N = 15$ (lower panel) at $b = 0.5$. The real part of P_1 is shown by [red] pluses and the imaginary by [blue] bursts. The values of κ are 0.148 in $SU(8)$, and 0.155 in $SU(10)$ and $SU(15)$.

hysteresis, indicative of a first-order transition. The average magnitude of the Polyakov loops, shown in the right panel, displays a much weaker hysteresis, with $\langle |P_\mu| \rangle \ll 1$ on both sides of the transition. Based on this, and on the behavior of the scatter plots of the P_μ and $M_{\mu\nu}$ (not shown), we conclude that this transition does not involve any breaking of the center-symmetry.

We next show, in Fig. 11, a compilation of all our $N = 8$ results for $b = 0.1$–1.0. We observe that, as b increases, the transition shifts to smaller values of κ and the discontinuity in the plaquette decreases. These two features are qualitatively consistent with expectations for the critical line $\kappa_c(b)$ in the first-order scenario discussed in Secs. II and III. In particular, we expect that the transition should

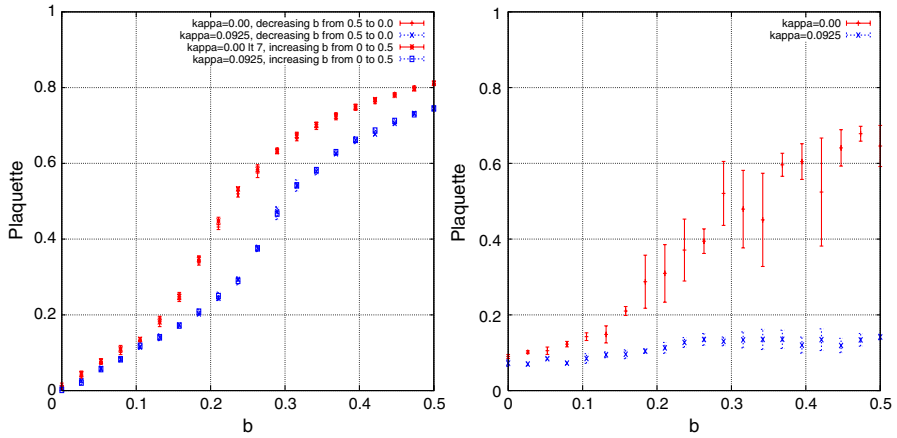

FIG. 9 (color online). Scans of the plaquette (left panel) and the magnitude of the Polyakov loop $P_{\mu=1}$ (right panel) for $N = 10$ at $\kappa = 0$ ([red] pluses) and $\kappa = 0.0925$ ([blue] crosses).

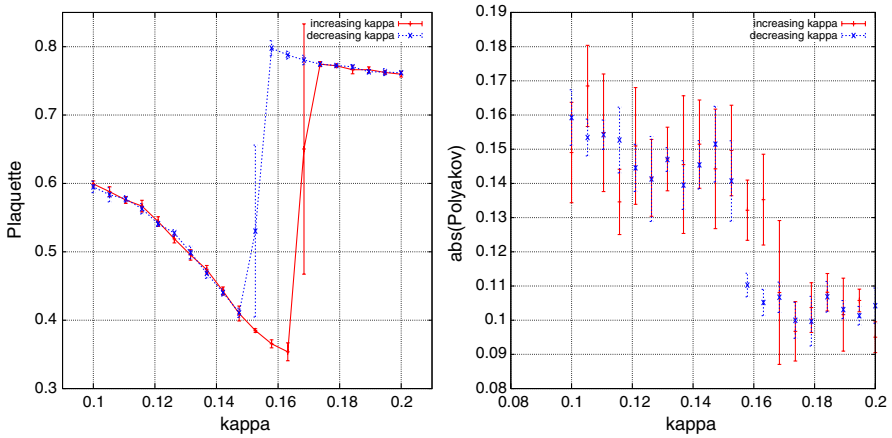

FIG. 10 (color online). Hysteresis scans in κ for $N = 8$ at $b = 0.35$, for the average plaquette (left panel) and the average magnitude of the Polyakov loops (right panel). Scans with increasing (decreasing) κ are shown using [red] pluses ([blue] crosses).

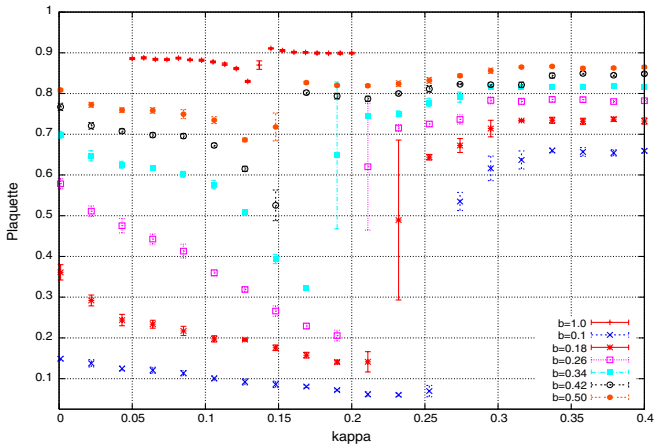

FIG. 11 (color online). Scans of the plaquette as a function of κ for $N = 8$ at $b = 0.1$, 0.18, 0.26, 0.34, 0.42, and 0.5.

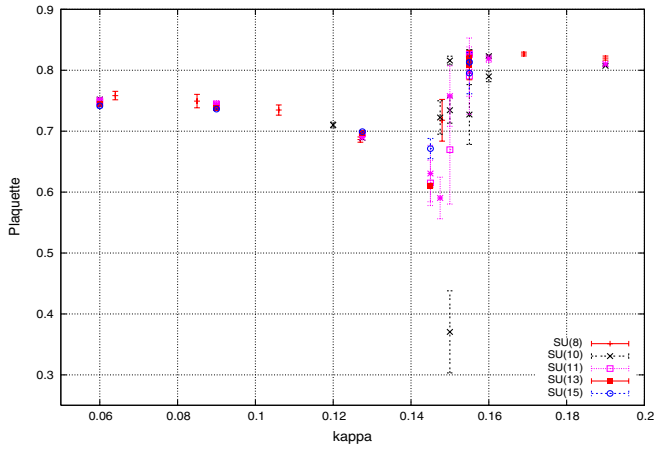

FIG. 12 (color online). The plaquette as a function of κ at $b = 0.5$ for $N = 8$, 10, 11, 13, and 15.

interpolate between $\kappa = 0.125$ at $b = \infty$ and $\kappa = 0.25$ at $b = 0$, and our results are consistent with this expectation.[9] We also expect that the transition should weaken rapidly as b increases, as observed.

It is also important to investigate the N dependence. If, when $N \to \infty$, there is a first-order transition, we would expect an increasingly wide region of metastability as N increases. We have studied this at $b = 0.5$ for $N = 8$, 10, 11, 13, and 15, with results shown in Fig. 12. We see only a very weak dependence on N away from the transition (indicating that our results for the plaquette are close to their $N = \infty$ values), while there is some evidence for increasing metastability as N increases. This is most notable for $N = 10$ ([black] crosses) compared to $N = 8$ ([red] pluses).

If our interpretation is correct, then the pions composed of adjoint quarks should have a minimal, nonzero mass along the critical line, and the long-distance physics on both sides of the transition should be the same. It is beyond the scope (and resources) of the present calculation to test these claims directly. Clearly this is an important issue for further work. In this regard, it is useful to convert our values of b into the corresponding values of β in a standard $SU(3)$ simulation with Wilson gauge and fermion action. The relation is $\beta = 2N^2 b$, so that $b = 0.35$, 0.5, and 1 convert to $\beta = 6.3$, 9, and 18, respectively. In pure-gauge simulations, one enters the weak-coupling regime at $\beta \approx 6$, and this crossover value is reduced by the presence of fermions. Consequently, our calculations at $b \geq 0.4$ are well inside the weak-coupling region.

[9]If there is an Aoki phase for small b this transition line would correspond to the position of the left-hand boundary of this phase. We have not done detailed studies at small b to elucidate a possible region of an Aoki phase.

It is interesting to compare the phase diagram we have found thus far to that observed for the large-volume $N_f = 2$, $N = 2$ theory in Ref. [29]. In scans of the plaquette versus κ, Ref. [29] shows a similar first-order transition for stronger couplings, but also finds that the line of such transitions ending at the point $b = \beta/8 \approx 0.25$, $\kappa \approx 0.19$. This is a very different behavior from that we have observed, consistent with the underlying physics being itself quite different.

E. Exploring larger κ values

We have also performed some scans at larger values of κ. Here we are outside the regime which is connected by reduction to physical QCD (which is roughly $0.05 \lesssim \kappa \lesssim 0.2$), but this region is interesting for several reasons. First, we want to determine the boundaries of the region in which the center symmetry is unbroken, so that reduction holds. We also want to make a connection with the one-loop computation of [14], which found a Z_N-symmetry-breaking transition for $\kappa \gtrsim 1.4$. Finally, it is simply interesting in its own right to understand the phase structure of this single-site model.

What we find is a complicated set of phase transitions, involving partial breaking of the center symmetry. These are reminiscent of the transitions found in the one-loop potential studies of Ref. [13]. We have not fully untangled the phase structure, and will thus only present a sampling of our results along with some conjectured interpretations.

As an example, in Fig. 13 we present scatter plots of the $M_{\mu,\pm\nu}$ observables (defined in Sec. V A), for $N = 10$ and $b = 0.5$. The value of κ varies from 0.0001 (where the theory is essentially pure gauge), through the intermediate values of κ discussed in Sec. V D, up to large values (by which we mean $\kappa \gtrsim 0.2$). The corresponding Polyakov loop scatter plots are presented in Fig. 14 (note that there is some overlap with Fig. 6). We observe that, for $\kappa \lesssim 0.2$, the $M_{\mu,\pm\nu}$ behave similarly to the Polyakov loops: they show center-symmetry breaking for $\kappa \simeq 0$ [if the links, U_μ, have phases close to $e^{2in_\mu\pi/N}$ then the $M_{\mu,\pm\nu}$ have phases close to $e^{2i(n_\mu \pm n_\nu)\pi/N}$], but then fluctuate around zero for intermediate values of κ, as exemplified by the results shown for $\kappa = 0.1275$. The fluctuations are, however, much larger for the $M_{\mu\nu}$ than for the Polyakov loops.

A new behavior is seen for $\kappa \gtrsim 0.2$. As illustrated by the results at $\kappa = 0.245$ and 0.275, the $M_{\mu\nu}$ show symmetry breaking (although with tunnelings between "vacua") while the P_μ do not. This indicates a mode of center-symmetry breaking involving the correlation of eigenval-

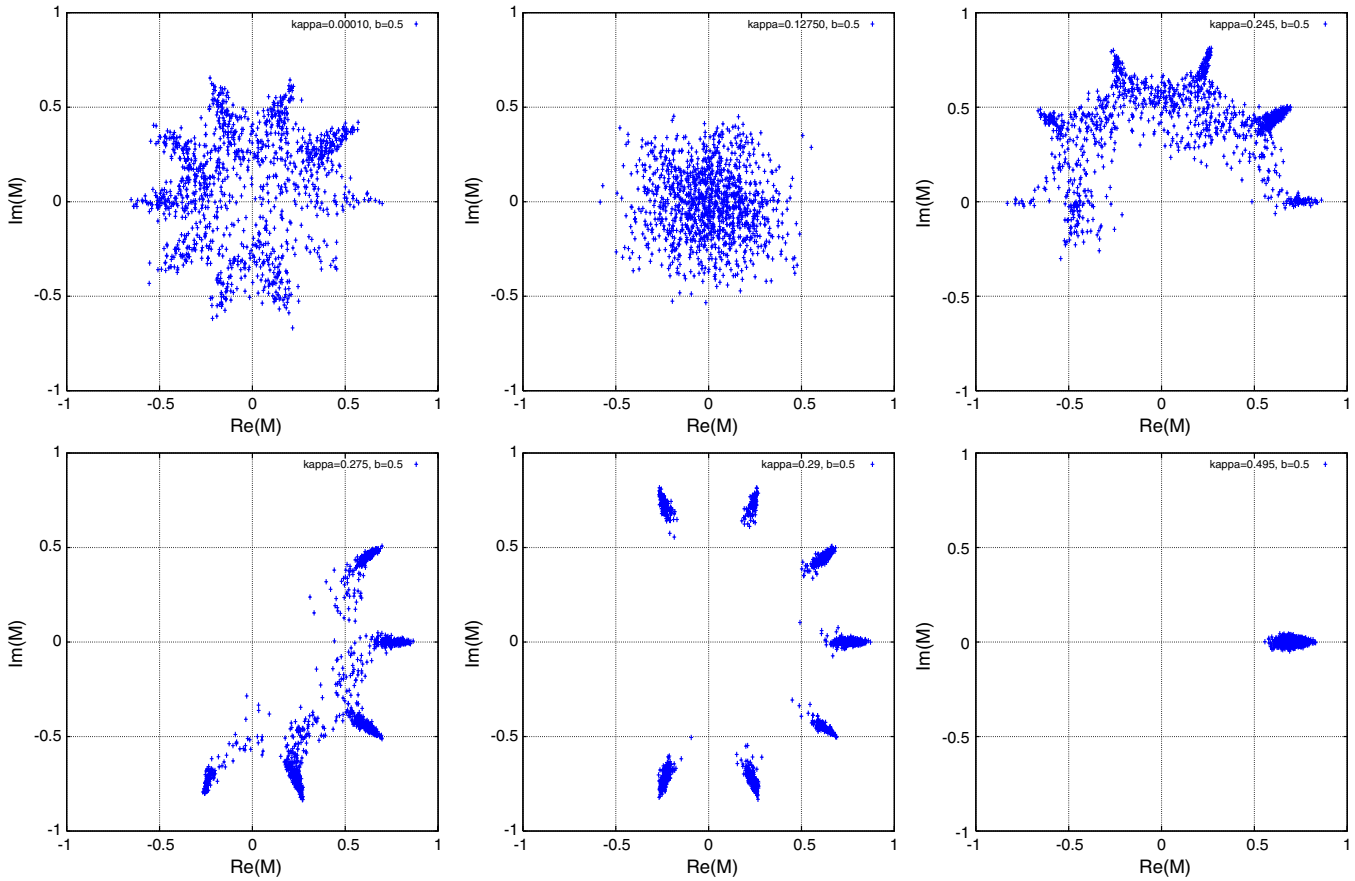

FIG. 13 (color online). Scatter plots of the 12 $M_{\mu,\pm\nu}$ for $N = 10$, $b = 0.5$. Here $\kappa = 0.0001$, 0.1275, 0.245, 0.275, 0.29, and 0.495 (running from top-left to bottom-right).

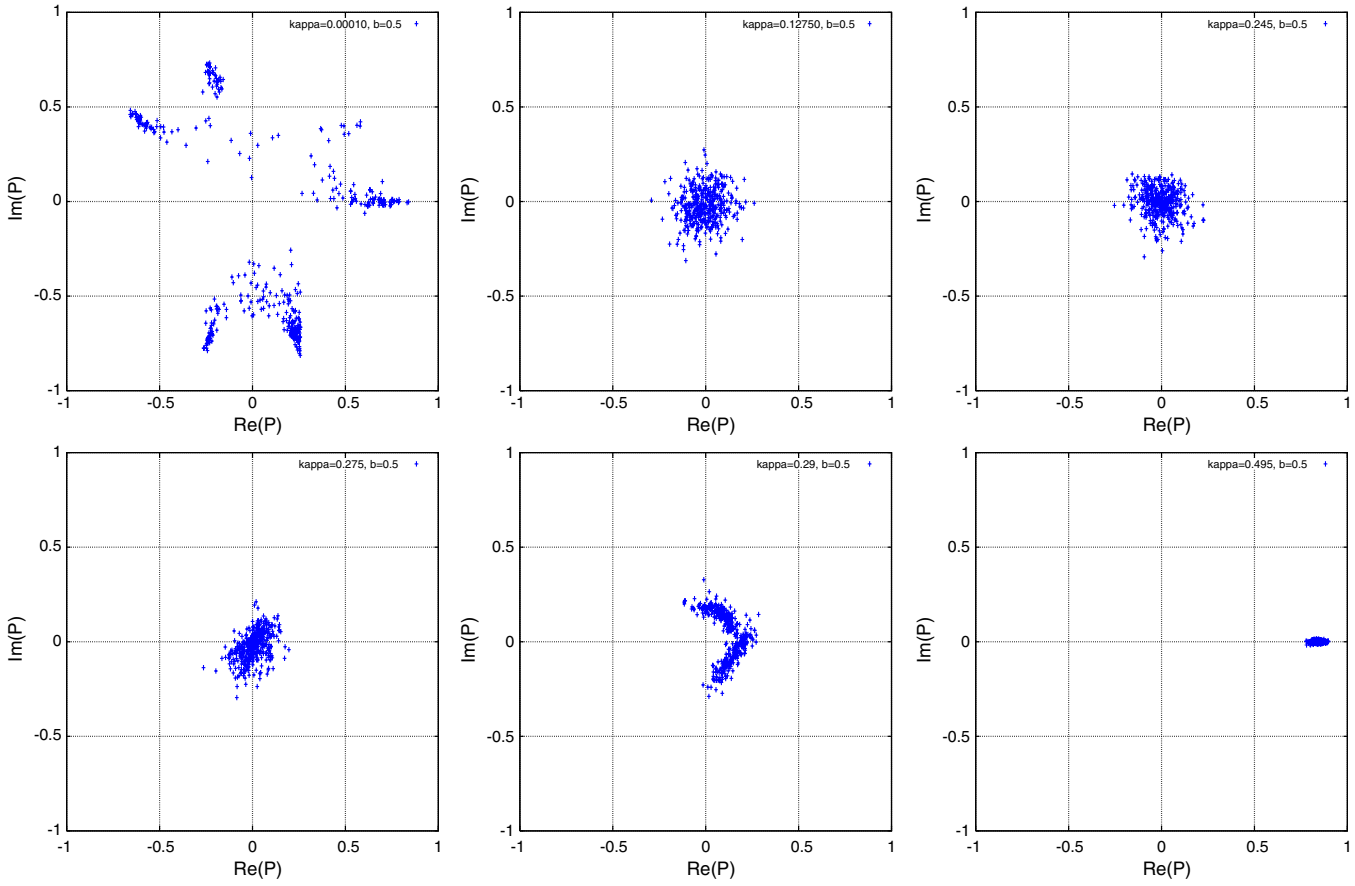

FIG. 14 (color online). Scatter plots of the four P_μ for the same data set as in Fig. 13.

ues of links in different directions, while the eigenvalues themselves remain uniformly distributed. This is the pattern we observed in the quenched EK model [24], and shows the importance of using order parameters other than the Polyakov loops.

The onset of this behavior is examined in more detail [now for $SU(11)$] in Figs. 15 and 16. The first two panels show the distribution of $M_{\mu\nu}$ spreading out, with some of the them having an almost fixed phase, while the P_μ remain close to the origin and show no signs of symmetry breaking. The bottom two panels in each figure show that, as κ is increased further, all the $M_{\mu\nu}$ show a clear symmetry-breaking pattern, while the P_μ start to move away from the origin. This is also seen in the penultimate panels of Figs. 13 and 14.

By studying the distribution of the individual P_μ and $M_{\mu\nu}$, we have determined a possible explanation for some of these scatter plots in terms of the behavior of the eigenvalues of the link matrices. As an example, consider the case of $N = 10$, $b = 0.5$, and $\kappa = 0.275$, shown in Figs. 13 and 14. At long Monte-Carlo time, when all the $M_{\mu\nu}$ are in the "points" of the "stars," they can be understood semiquantitatively if

$$U_\mu \approx e^{2\pi i n_\mu/10}\mathrm{diag}(i, i, i, i, i, -i, -i, -i, -i, -i) \times \text{fluctuations}, \tag{5.2}$$

with $n_1 = n_4 = 1$ and $n_2 = n_3 = 2$. The order of the diagonal elements in U_μ is unimportant, but must be the same for all four links. Note that the matrix in Eq. (5.2) does have unit determinant as required to be in $SU(10)$, but is traceless and so leads to vanishing P_μ. Fluctuations reduce the magnitude of the $M_{\mu\nu}$ from unity down to about 0.75, and lead to the P_μ spreading out around the origin. Thus one can understand the behavior for these order parameters as due to the eigenvalues clumping into two subsets [thus breaking the symmetry down to $(Z_2)^4$], *and* the "locking" of the eigenvalues of the different links (breaking the symmetry further down to Z_2). Note that the precise form of the eigenvalue clumping is dependent on N. For example, the form in Eq. (5.2) cannot be generalized to odd N, for which one eigenvalue is "left out." This can be used to understand why the P_μ in the last two panels of Fig. 16 (for which $N = 11$) are not centered on the origin.

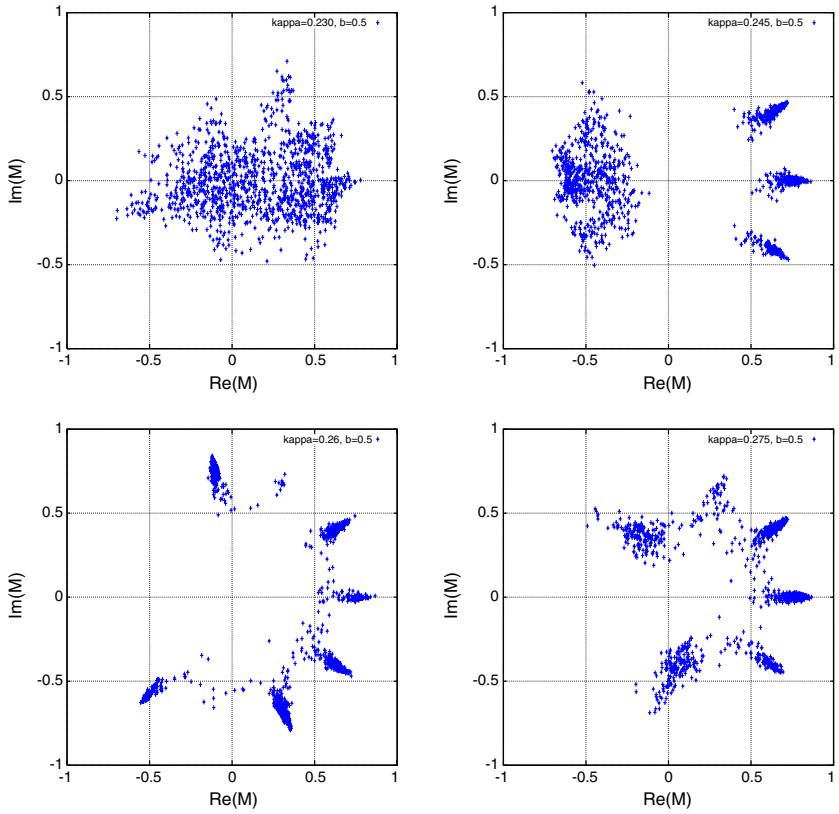

FIG. 15 (color online). Scatter plots of the $M_{\mu,\pm\nu}$ for $N = 11$ and $b = 0.5$. Here $\kappa = 0.23$, 0.245, 0.26, and 0.275 (running from top-left to bottom-right).

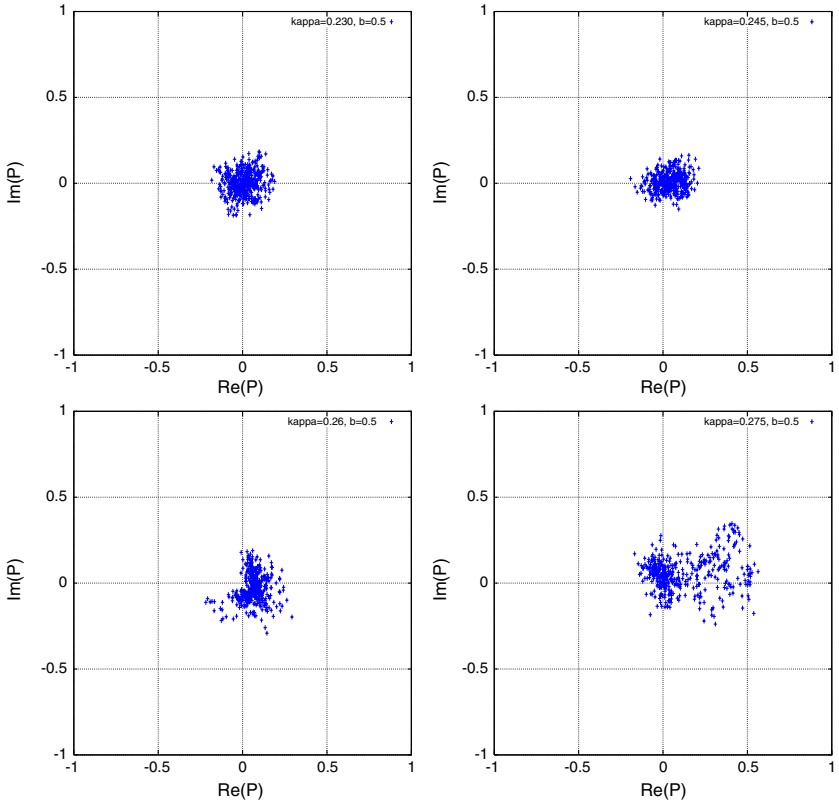

FIG. 16 (color online). Scatter plots of the P_μ for the same data set as in Fig. 15.

As κ is increased further, there is another transition (or transitions) to a phase (or phases) in which both the $M_{\mu\nu}$ and the P_μ show symmetry breaking (as illustrated by the last panel of Figs. 13 and 14). We have also observed a significant dependence on initial conditions in this region.

In summary, there is a complicated phase structure for $\kappa \gtrsim 0.2$, the details of which depend on N. For our purposes, however, the important conclusion is that, in this region, the center symmetry is broken, and so reduction fails. Thus we have not attempted a thorough study of this region.

We close this subsection by comparing our results to those from the 1-loop calculation of Ref. [14]. The latter finds that the center symmetry is broken only for $\kappa \gtrsim 1.4$, a much larger value than that we find in the single-site model. This large difference may simply be due to the difference in the geometries: a single short direction versus four short directions. It may also be because Ref. [14] only estimated energies of simple vacua such as those corresponding to an unbroken Z_N symmetry or a completely broken Z_N symmetry. The transition at $\kappa \simeq 0.04$ corresponds to such a breaking, and indeed seems to agree with the one-loop result. In contrast to this, the transitions at $\kappa \gtrsim 0.2$ involve a more complicated breaking of the symmetry, which was not studied in [14].

F. High statistics study of center-symmetry realization for $0.05 \lesssim \kappa \lesssim 0.2$

In this section we perform more stringent tests to check whether the center symmetry is intact in the physically interesting regime $0.05 \lesssim \kappa \lesssim 0.2$. One motivation for doing so comes in part from the examples seen in the previous subsection. There we saw that simply looking at the Polyakov loops is insufficient because the center symmetry can be only partially broken. Thus it is important to use a set of order parameters sensitive to a range of different patterns of symmetry breaking. Another motivation is to push the calculation to couplings weaker than $b = 0.5$, so as to see if there is any barrier to taking the continuum limit in the phase in which reduction holds. In other words, we would like to study whether the central funnel in Fig. 2 continues up to larger b. Finally, we are concerned that the runs discussed so far might be too short to resolve the equilibrium state of the theory for some choices of parameters. For example, the time histories shown in Fig. 8 indicate rather long decorrelation times at $b = 0.5$. One

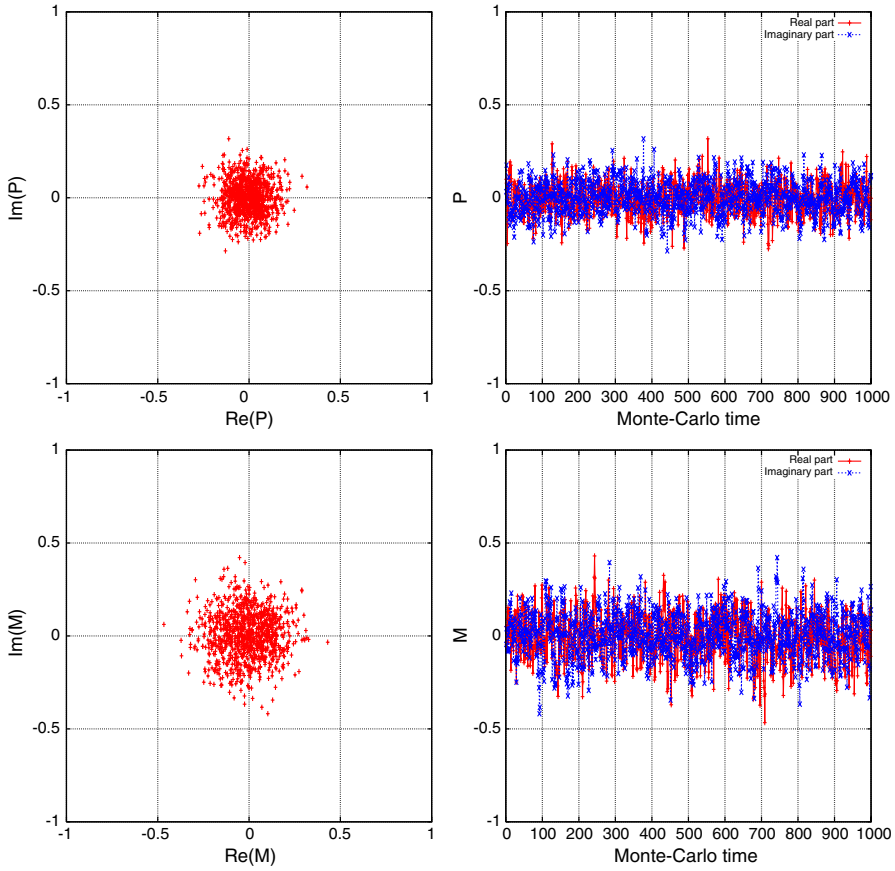

FIG. 17 (color online). Scatter plots (left panels) and Monte-Carlo time histories (right panels) of 1000 measurements of P_1 (upper panels) and $M_{2,1}$ (lower panels), for $N = 10$, $b = 0.35$, and $\kappa = 0.155$. In the right panels, [red] pluses show the real part, while [blue] crosses show the imaginary part.

would expect this problem to worsen as b increases, and indeed we find decorrelation times of $O(50)$ (as estimated by eye) at $b = 1.0$. We also find qualitative evidence that decorrelation times increase as one approaches κ_c.

In order to attempt to address these concerns we performed several long runs, listed in Table II, consisting of 1000–3500 measurements. We begin with a case in which the symmetry-breaking pattern should be "easy" to resolve based on the results given in previous subsections: the $SU(10)$ theory at $b = 0.35$ and $\kappa = 0.1275$. This is well within the funnel and yet not close to κ_c. Examples of the scatter plots and time histories are shown in Fig. 17. It appears that these runs are long enough to unambiguously see that P_1 and $M_{2,1}$ (and the other $P_{\mu\nu}$ and $M_{\mu\nu}$, for which the plots are similar) are fluctuating around zero. This is consistent with the conclusion drawn above, namely, that the center symmetry is intact for these values of b and κ.

We now move to weaker coupling. The decorrelation time increases noticeably at $b = 0.5$ (not shown), although the evidence for the absence of symmetry breaking remains strong. By the time one reaches $b = 1.0$, however, the results do not have such a clear-cut interpretation. This is illustrated in Fig. 18, which shows results at a value of κ chosen to be in roughly similar relation to κ_c as that used in Fig. 17, so that the quark masses are roughly comparable. The scatter plots are not symmetric about the origin, and it is difficult to tell from these results alone whether this indicates simply that the run is too short or whether the large fluctuations in the time histories are in fact tunneling events between different phases in which the symmetry is broken. We think the former possibility more likely, but the latter should be kept in mind at this stage.

One way to differentiate between these two interpretations is to study how the fluctuations depend on N. If the symmetry is intact, then $\langle |P_\mu|^2 \rangle$ and $\langle |M_{\mu,\nu}|^2 \rangle$ should vanish as $1/N^2$ as $N \to \infty$. If, instead, the symmetry is broken, they should tend to a finite value, with $1/N^2$ corrections. We have tried to make this test by comparing $SU(10)$ and $SU(13)$ runs at $b = 1.0$, $\kappa = 0.09$. An example is shown in Fig. 19. The fluctuations do decrease as N increases, with $\langle |M^2_{\mu,\nu}| \rangle$ dropping from 0.0850(28) to 0.0620(25). If we rely on these two values, then extrapolating in $1/N^2$ to $N = \infty$ yields 0.023(11). This is consistent with no symmetry breaking.

Another option for studying symmetry breaking is to study expectation values of the operators $K_{\vec{n}}$, defined in Sec. V A. Since there are a large number ($\sim 10^4$) such observables, we have to find an efficient way to present the results. We proceed by determining the signal-to-noise ratio for each $\vec{n}$:

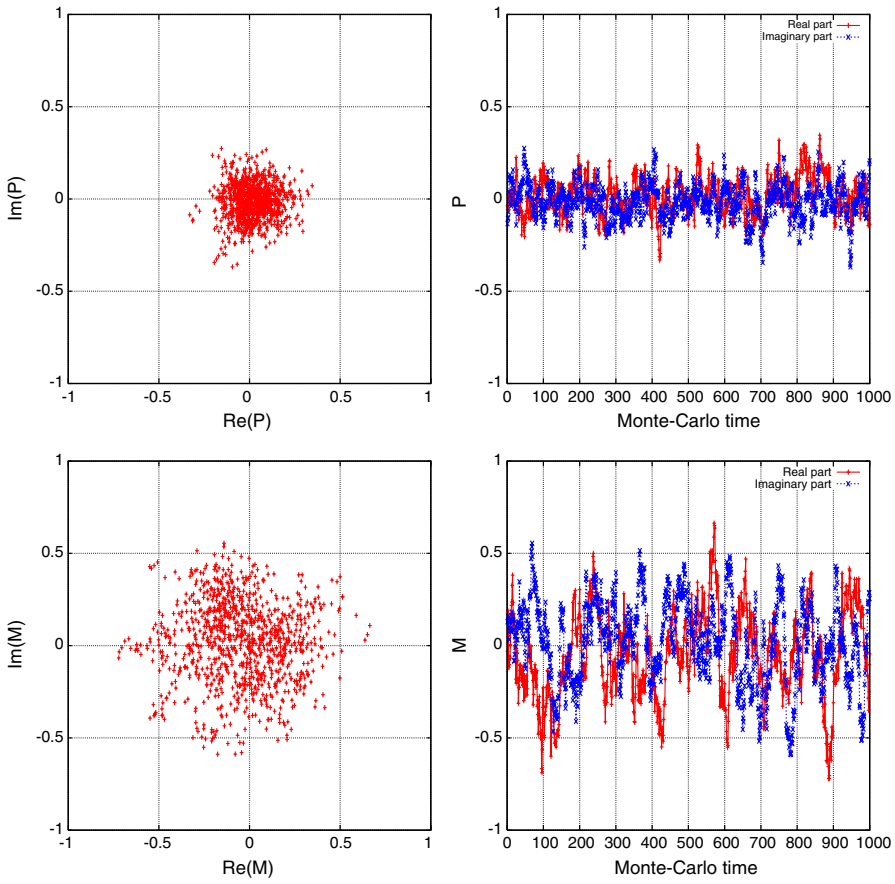

FIG. 18 (color online). As in Fig. 17 but for $b = 1.0$ and $\kappa = 0.1275$.

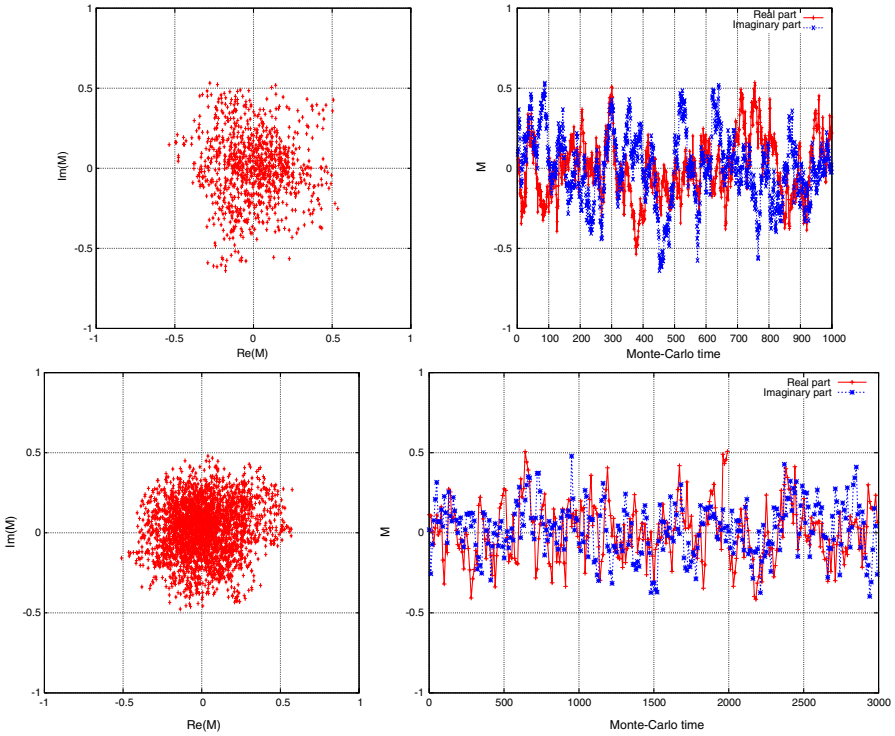

FIG. 19 (color online). As in Fig. 17, but showing $M_{2,1}$ only, and for $b = 1.0$, $\kappa = 0.09$. Upper and lower panels show, respectively, results for $N = 10$ (1000 measurements) and $N = 13$ (3000 measurements—only every tenth being shown).

$$r_{\vec{n}} = \frac{\langle K_{\vec{n}} \rangle}{\Delta K_{\vec{n}}}, \tag{5.3}$$

(where $\Delta K_{\vec{n}}$ is the error in $K_{\vec{n}}$). If the $(Z_N)^4$ symmetry is unbroken, all the expectation values should be consistent with zero within errors. Thus we expect $r_{\vec{n}}$ to be distributed approximately as a Gaussian with width ~ 1. We do not expect an exact Gaussian because we are working at finite N and because the observables $K_{\vec{n}}$ are correlated. Nevertheless, if there is symmetry breaking, and some of the observables have nonzero expectation values, we expect outliers with $|r_{\vec{n}}| \gg 1$. Thus we study many possible realizations of the $(Z_N)^4$ symmetry by looking at the histogram of the $r_{\vec{n}}$. Note that since $K_{\vec{n}}$ is a complex number, we perform this analysis for both its real and imaginary part, and denote the corresponding ratio and histograms by $r_{\text{real,imag}}$ and $H(r_{\text{real,imag}})$.

We begin showing in Fig. 20 the histograms $H(r_{\text{real}})$ for two choices of parameters where we know what to expect. These are

(i) $SU(10)$ at $b = 0.35$ and $\kappa = 0.1275$ (1000 measurements), for which all the evidence discussed above strongly suggests that the Z_N symmetry is intact (see, for example, Fig. 17).

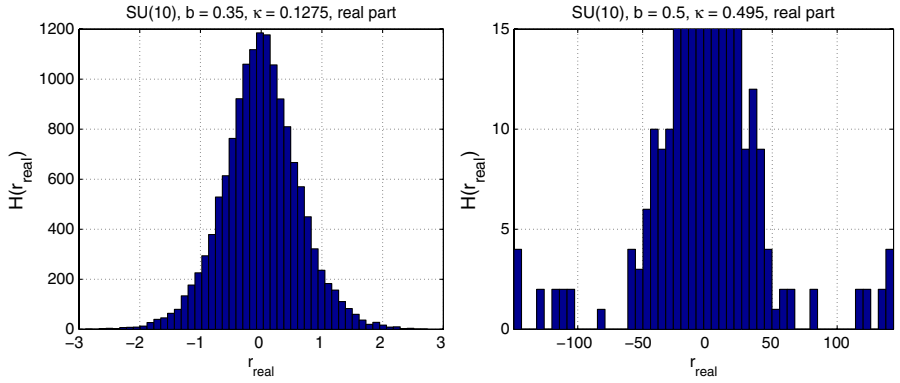

FIG. 20 (color online). Histograms of the signal-to-noise ratio of the real part of $K_{\vec{n}}$. *Left*: A case where the center-symmetry is intact ($N = 10$, $b = 0.35$, $\kappa = 0.1275$). *Right*: A case where the symmetry is broken ($N = 10$, $b = 0.5$, $\kappa = 0.495$), with the top of the histogram cutoff.

(ii) $SU(10)$ at $b = 0.5$ and $\kappa = 0.495$ (100 measurements), where we have strong evidence that the Z_N symmetry is broken (see the bottom-right panels of Figs. 13 and 14).

For the first choice (left panel) we see the expected Gaussian-like distribution, with almost all observables consistent with zero within 2σ. By contrast, for the second choice (right panel), there are many traces whose signal-to-noise ratio is very large, of $O(100)$. This is a clear indication that the symmetry is broken (and the pattern of breaking can be deduced by determining for which $\vec{n}$ the signal is significant).

Now that we have confidence in this method, we apply it to cases where the symmetry realization is less clear. Examples of the results are collected in Fig. 21. Here the top row shows $H(r_{\text{real}})$ at $b = 0.35$ and $N = 10$ as we approach closer to κ_c (which, from Fig. 11, is at ≈ 0.175), and should be compared to the left panel of Fig. 20. The middle row of Fig. 21 shows $H(r_{\text{real}})$ at weaker coupling ($b = 1.0$, still $N = 10$) both away from ($\kappa = 0.09$) and close to ($\kappa = 0.1275$) κ_c. These are from the same data sets as those illustrated in the upper panels of Fig. 19, and all panels of Fig. 18, respectively. Finally, the bottom row shows $H(r_{\text{real}})$ and $H(r_{\text{imag}})$ (left and right panels) at $b = 1.0$, $\kappa = 0.09$, but now at $N = 13$ (corresponding to the data in the lower panels of Fig. 19).

In none of these cases is there any evidence for outliers, and we conclude that it is unlikely that the center symmetry breaks in the funnel region, at least up to $b = 1.0$. We note

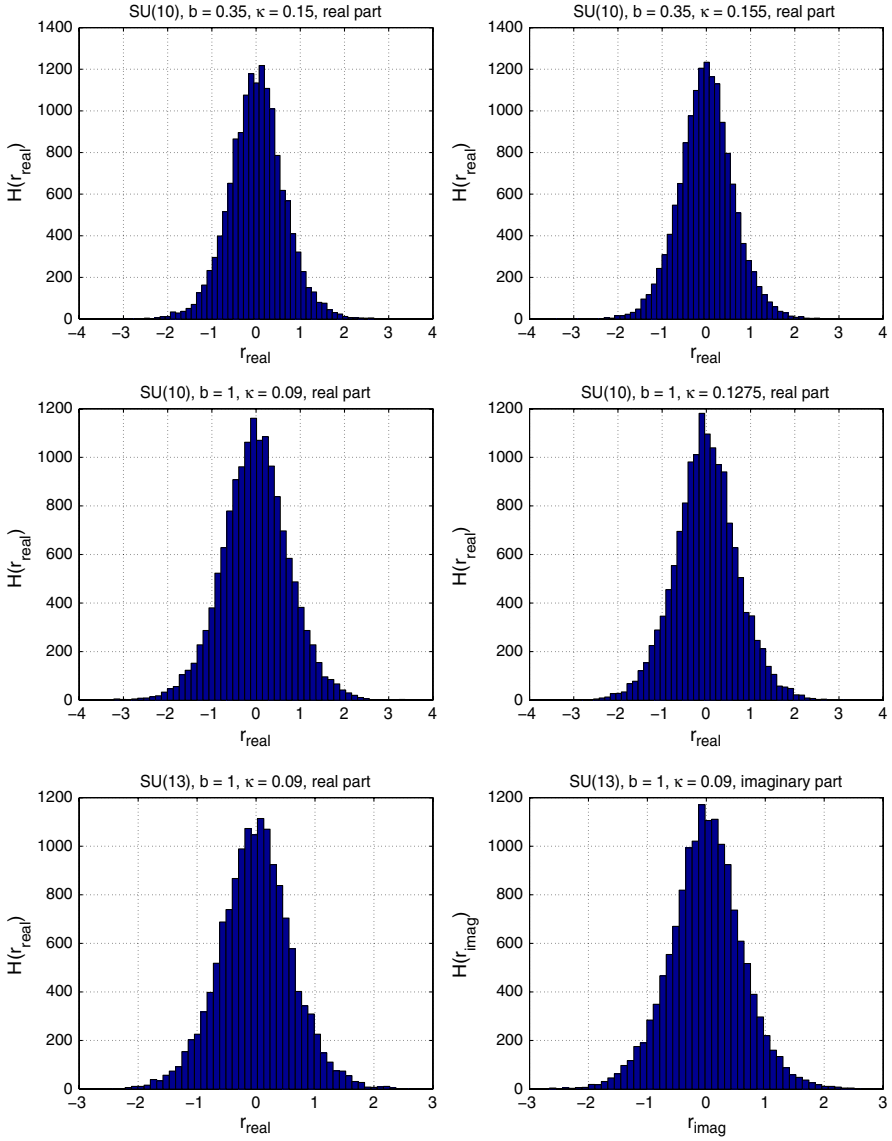

FIG. 21 (color online). Histograms of $r_{\vec{n}}$ for various parameters of interest. From top-left to bottom-right, parameters are (i) $N = 10$, $b = 0.35$, $\kappa = 0.150$ (real part), (ii) $N = 10$, $b = 0.35$, $\kappa = 0.155$ (real part), (iii) $N = 10$, $b = 1.0$, $\kappa = 0.09$ (real part), (iv) $N = 10$, $b = 1.0$, $\kappa = 0.1275$ (real part), (v) $N = 13$, $b = 1.0$, $\kappa = 0.09$ (real part), (vi) $N = 13$, $b = 1.0$, $\kappa = 0.09$ (imaginary part).

TABLE III. Comparison of plaquette expectation values u of large-N pure-gauge theory with those obtained in our single-site simulations.

b	u	κ	$SU(8)$	$SU(10)$	$SU(11)$	$SU(13)$	$SU(15)$
0.5	0.718	0.09	0.7460(20)	0.7429(20)	0.7420(12)	0.7388(22)	0.7362(12)
0.5	0.718	0.1275	0.6836(12)	0.6877(7)	0.6959(18)	0.6974(18)	0.6992(16)
1	0.870	0.09	0.883 04(10)	0.8700(4)	0.8798(14)	0.8779(6)	0.8774(8)

that this histogram method appears to be a more powerful tool than looking at individual scatter plots and time histories.

VI. RESULTS OF PHYSICAL INTEREST

Having found evidence that reduction holds in the interesting region on either side of the putative critical κ, we now make a first attempt at extracting quantities of physical interest. As $N \to \infty$, the results we find should hold also for the large-N infinite-volume gauge theory with one adjoint quark (as long as one uses the same action and the same values of b and κ). As κ approaches κ_c, the quarks become light, and their contribution to the dynamics becomes important. Conversely, as κ moves away from κ_c (towards zero, say), the quarks become heavy (compared to its dynamically generated scale) and the dynamics approaches that of the pure-gauge theory. The fact that reduction appears to hold down to small values, $\kappa \approx 0.05$, where we expect the quarks to be very heavy, indicates that we may well be able to use reduction to study the pure-gauge theory using this ''adjoint deformation.''

What we would like to do is use known results from the infinite-volume pure-gauge theory to see how close we are to $N = \infty$.[10] Unfortunately, we cannot do any quantitative comparisons at this stage. For one thing, since we are at this stage unable to measure pion masses, we do not know where the boundary between light and heavy quarks lies. And even if we had determined that the quarks are heavy, so that the long-distance physics was that of the pure-gauge theory, the presence of a nonzero κ would lead to additional terms in the gauge action, including, for example, the trace of the plaquette in the adjoint representation. In other words, reduction would match our single-site model to a pure-gauge theory with a different gauge action, with the additional terms entering at $O(\kappa^4)$.

Despite these drawbacks, we think it useful to attempt a large-N extrapolation for some quantities in order to make a qualitative comparison to the pure-gauge theory. We do so for the average plaquette and for the distribution of eigenvalues of a quenched overlap fermion in the fundamental representation. We also attempted to extract the string tension from the $e^{-A\sigma}$ dependence of Wilson loops, with A the area. (The loops are calculated using the reduction prescription of Ref. [2].) We find that the Wilson-loop expectation values do drop as A increases, but only for a short window, $A < A_c$, after which they start to grow. This growth is presumably due to $1/N$ corrections. Although we find that the upper edge of the window, A_c, grows with N, the window is too small at our values of N to extract a string tension. This problem could be resolved either by using larger values of N or by developing variational techniques to extract the tension at short distances. We leave this for future studies.

A. Average plaquette

We begin by comparing the values of the plaquette. We focus on three (b, κ) values at which we have good statistical control for $N = 8$–15: (0.5, 0.09), (0.5, 0.1275), and (1, 0.09). The results are collected in Table III. We also include in the table the value for the pure-gauge theory in the large N limit. For $b = 0.5$ this is given by [44][11]

$$u(\kappa = 0, b = 0.5) \simeq 0.7182, \tag{6.1}$$

while for larger values of b, we use three-loop perturbation theory (taken from, for example, Ref. [22])

$$u(\kappa = 0, b) \overset{b\to\infty}{\to} 1 - \frac{1}{8b} - \frac{0.653\,687}{128b^2} - \frac{0.406\,640\,6}{512b^3} + \ldots \tag{6.2}$$

$$= 0.8692\ldots \quad \text{at } b = 1.0. \tag{6.3}$$

At $b = 1.0$ the $1/b^3$ term contributes about 0.1% to the plaquette value and so we estimate the error in the result to be ~ 0.0008.

What we see is that the results at $\kappa = 0.09$ (for both values of b) approach the pure-gauge theory value from above as $N \to \infty$, while that at $\kappa = 0.1275$ (where the quark mass is lighter) approaches from below. To see how close they approach this value, and to study the nature of the $1/N$ expansion, we fit our data to

$$u(N) = u(\infty) + \frac{A}{N^q}, \quad \text{with} \quad q = 1 \quad \text{or} \quad 2. \tag{6.4}$$

[10] We are not aware of any results for the large-volume gauge theory with $N_f = 1$ dynamical adjoint quarks with which to compare.

[11] The error on this number is very small and we can safely assume that it is zero in the discussion below.

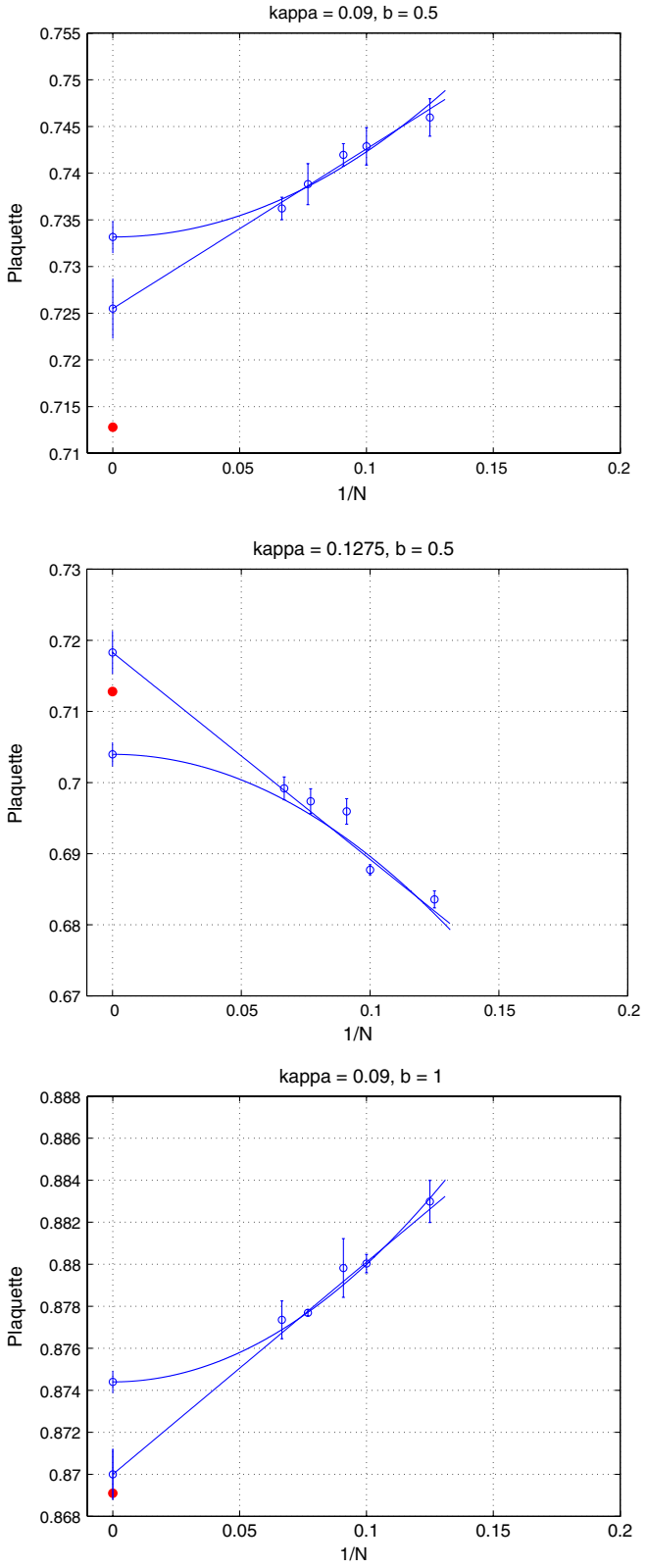

FIG. 22 (color online). Large-N extrapolations of the average plaquette for $(b, \kappa) = (0.5, 0.09)$, $(0.5, 0.1275)$, and $(1.0, 0.09)$ (running from top to bottom). The filled circle [red] at $N = \infty$ is u, the value in the large-N limit of the infinite-volume pure-gauge theory.

The $1/N^2$ fit is appropriate if we are in the asymptotic regime, while the $1/N$ fit is an attempt to mock up the behavior if we are far from asymptotia. The resulting extrapolations are shown in Fig. 22, with fit parameters given in Table IV. We observe that the linear and quadratic fits are of comparable quality, indicating that we need a wider range of N to pin down the appropriate fitting form. One can perhaps use the difference between these fits as a crude estimate of the extrapolation uncertainty. The rather large χ^2 values in the second row of the table reflect the scatter of our data around the fit lines (see Fig. 22) and might indicate underestimated statistical errors or a competition between multiple terms in the $1/N^2$ expansion.

As noted above, reduction does not predict that the extrapolated single-site plaquette values should agree with those in the pure-gauge theory at infinite volume, only that they should be close for small κ. It is therefore slightly surprising that we find better agreement for $\kappa = 0.1275$ than for 0.09 at $b = 0.5$. Further work will be required to determine the significance of this finding.

B. Dirac spectrum of fundamental fermions

One drawback of the average plaquette is that its value is dominated by short-distance physics (i.e. gauge fluctuations with wavelengths $\sim 1/a$). We consider in this section a quantity that is sensitive to long-distance physics, and thus serves as a better test of whether our values of N are large enough to extract long-distance quantities.

The idea, proposed in Ref. [45], is to probe the large-N theory using the eigenvalue spectrum of valence fermions in the fundamental representation. As discussed in Ref. [45], it is legitimate in this context to quench fundamental representation fermions in the large-N limit.[12] The specific proposal is to calculate the distribution of the low-lying eigenvalues of the quenched overlap Dirac operator and compare them to the predictions of random-matrix theory (RMT). This constitutes a test that the chiral-symmetry-breaking dynamics of large-N QCD are being correctly reproduced, because the RMT predictions can be derived from QCD if the eigenvalues are in the so-called "epsilon-regime" and if some other conditions hold [47]. One can furthermore extract a value for the condensate, $\langle \bar{q}q \rangle / N$, from this comparison.

This approach is used in Ref. [45] in the context of partial volume reduction, in which one simulates $SU(N)$ pure-gauge theories in boxes of physical size of $O(1\ \mathrm{fm})$, which are found to be large enough to satisfy volume independence [18]. It is argued in Ref. [45] that the eigenvalue densities of the valence Dirac operator of the (partially) reduced theory are legitimate quantities to be compared with those of RMT as long as N is large enough. Specifically, one should expect that the smallest eigenval-

[12] See Ref. [46] for further discussion of the conditions under which such quenching is, and is not, justified.

TABLE IV. Results of extrapolations of plaquette to $N = \infty$, obtained from fitting the data in Table III to the form Eq. (6.4).

Data set	Type of fit	$u(\infty)$	A	χ^2/d.o.f.
$b = 0.5$, $\kappa = 0.09$, $u = 0.718$	Linear	0.7255(32)	0.171(37)	1.45/1
	Quadratic	0.7332(17)	0.91(20)	1.1/1
$b = 0.5$, $\kappa = 0.1275$, $u = 0.718$	Linear	0.7183(30)	−0.291(30)	12/3
	Quadratic	0.7085(16)	−1.43(15)	16/3
$b = 0.5$, $\kappa = 0.09$, $u = 0.870$	Linear	0.8700(12)	0.101(16)	0.97/3
	Quadratic	0.8744(5)	0.559(77)	0.64/3

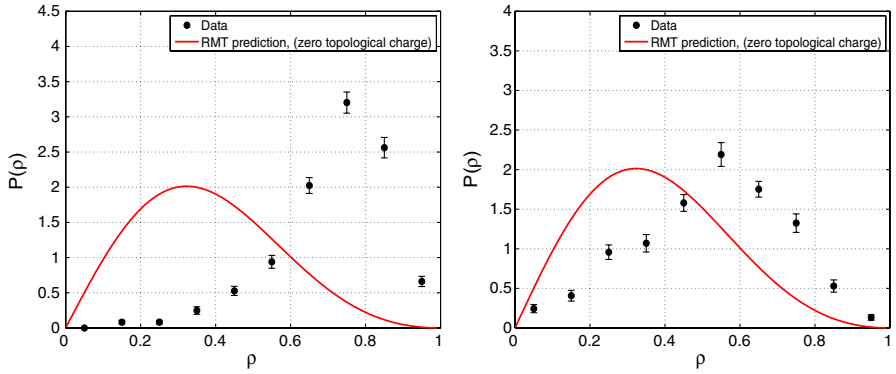

FIG. 23 (color online). The quantity $P(\rho)$ (see text) for $SU(10)$ and $b = 0.35$ compared to RMT (solid curves). The values of κ are 0.1275 (left panel) and 0.155 (right panel).

ues are described by RMT once NL^2 is large enough. This can be achieved either by increasing L or by increasing N.

A particularly useful quantity considered in Ref. [45] was the distribution, $P(\rho)$, of the ratio between the first and second eigenvalues of the overlap Dirac operator. This has the advantage, compared to the distributions of individual eigenvalues, that the RMT prediction is parameter free (i.e. is independent of the value of the condensate). Thus it can be used as a gauge of whether NL^2 is large enough. Indeed, using this quantity, Ref. [45] found that the measured $P(\rho)$ agrees with the RMT prediction on an $L = 6$ lattice only for $N \gtrsim 23$. In our case we have $L = 1$ and so we probably need even larger values of N in order to see the $P(\rho)$ asymptote to the its RMT form. Note that this expectation is justified only for values of κ that correspond to adjoint fermions heavier than the dynamical scale of the gauge theory. If the adjoint fermions become light, then their determinant will alter the expected distribution.

We thus calculate $P(\rho)$ for valence overlap fermions (using the conventions of Ref. [45], and taking $M_0 = -1.5$). Since the dimension of the Dirac matrix of the fundamental fermions is modest, 36–60, we can construct it exactly, without approximating the sign function involved in its definition. The parameters for which we calculated $P(\rho)$ were $N = 10$, $b = 0.35$ and $\kappa = 0.1275$, 0.155. These we expect to correspond to relatively heavy and moderately light fermions, respectively, based solely on their proximity to $\kappa_c \approx 0.175$. We used 1000 gauge configurations, all of which we found to have zero topological charge (using the index theorem).[13] We present our results for $P(\rho)$ in Fig. 23, together with a solid curve that is the analytic formula of RMT reproduced from Ref. [45].

The disagreement between our data and the RMT prediction is clear. The form of the disagreement is, in fact, similar to that seen in Ref. [45] for small values of N. This leads us to conclude our values of N are too small for the lowest two eigenvalues to be in the epsilon regime. It would be of considerable interest to extend this calculation to larger N.

Another obvious step is to perform a comparable study with a Dirac operator of a fermion in the adjoint representation. A straightforward generalization of the arguments in Ref. [45] shows that to be in the epsilon regime now requires N^2L^2 to be large enough, which is easier to satisfy, and it may be that our modest values of N suffice. One complication is that our fermion action, which uses the Wilson-Dirac operator, does not preserve chiral symmetry, so that we cannot make a direct comparison with RMT unless we include lattice artifacts. It may be possible to use the approach of Ref. [48], however, to study the condensate. It also may be possible to use a valence overlap operator for the adjoint fermions.

[13]We found that a few configurations had $|Q_{\text{top}}| = 1$ if we changed M_0.

VII. SUMMARY, CONCLUSIONS AND FUTURE DIRECTIONS

In this paper we have taken a step towards exploring large-N QCD with fermions in two-index representations. In these theories the number of both gauge *and* fermionic degrees of freedom grows as $O(N^2)$, so that the latter contribute to the dynamics even when $N \to \infty$. We do not study these theories directly, but rather use large-N equivalences to relate them to a much simpler theory, QCD with adjoint fermions defined on a single site. These equivalences follow from a combination of orbifold and orientifold projections [6]. Specifically, we choose to work with a single Dirac adjoint fermion which, through these projections, corresponds to a gauge theory with two Dirac fermions in the antisymmetric representation. For $N = 3$ the latter theory becomes physical (3-color) QCD with two degenerate Dirac fermions in the fundamental representation, and this makes our study relevant phenomenologically.

Clearly, for our approach to work it is necessary that the above-noted equivalences hold. This in turn requires that the ground state of the reduced theory is symmetric under the $(Z_N)^4$ center symmetry of the theory. The present paper is focused on determining, using Monte-Carlo simulations, the regime in the parameter space of the single-site theory within which the center symmetry remains unbroken. Our simulations were performed with $8 \leq N \leq 15$ at a variety of lattice spacings and quark masses. The observables we measure include order parameters for the breaking of $(Z_N)^4$ symmetry, and in some instances we gather large data samples, allowing the calculation of $\sim 10^4$ different order parameters that probe many potential patterns of symmetry breaking.

We find strong evidence that the center symmetry is intact in an extended region of the lattice parameter space, a region that includes the critical line along which we expect that the fermions have their minimum mass. Our results for the phase diagram depend very weakly on N, suggesting that they apply also when $N \to \infty$. In particular, the relatively small values of N that we use appear large enough to observe the first-order transition line at κ_c, despite the fact that this becomes a true transition only when $N \to \infty$. Our results are consistent with the region of unbroken center symmetry extending toward the continuum limit, so that the phase diagram is consistent with that conjectured in Fig. 2, although we cannot rule out that this region shrinks when $b > 1$.

An important finding is that the center symmetry does not break until the physical fermion mass becomes very heavy, likely at the cutoff scale (in approximate agreement with the analytic estimate Ref. [14]). For example, at $b = 0.5$, where $\kappa_c \approx 0.15$, the symmetry is unbroken for $\kappa = 0.06$ (see Figs. 6 and 7), so $m = (Z_m/a)[1/(2\kappa) - 1/(2\kappa_c)] \approx (Z_m/a) \times 5$. Since we expect $Z_m \sim O(1)$, the fermion mass is of $O(1/a)$. Thus there appears to be an overlap of the region in which reduction holds and that in which the long-distance physics of the corresponding large-volume theory is that of large-N pure-gauge theory. This finding opens a window to the study of the pure-gauge theory using reduction, which was the original idea behind the proposal of Eguchi and Kawai [2]. It seems likely that what is happening here is that the heavy fermions would, if integrated out, induce a tower of interactions between Polyakov loops that is similar to the tower of double-trace interactions proposed in Ref. [12] to stabilize the center symmetry.

As already noted, our evidence for the absence of center-symmetry breaking becomes less strong at the smallest coupling we consider, $b = 1.0$. This is an extremely small coupling, corresponding to $\beta = 18$ if $N = 3$. It is much smaller than the values for which we envision performing useful measurements of physical observables ($b \approx 0.35$). The issues that arise at $b = 1.0$ are that there are large fluctuations in Monte-Carlo time histories, and long autocorrelation times, making it hard to unambiguously determine the equilibrium state. It is for these couplings that the use of the $\sim 10^4$ order parameters becomes particularly useful, allowing us to try to tease out evidence of symmetry breaking. We find none.

A general lesson we have learned is that, when shrinking more than one Euclidean direction, the center symmetry sometimes breaks in quite nontrivial ways. For example, in some parts of the lattice phase diagram we observed ground states for which the expectation values of the Polyakov loop are consistent with zero, while other order parameters, which measure correlations between different Euclidean directions, have nonzero averages. This is similar to the behavior we observed in the quenched Eguchi-Kawai model [24], and shows that it is insufficient to measure only Polyakov loops (or any power thereof) when studying center-symmetry breaking.

Of course, finding that reduction holds is only the first step. Our ultimate aim is to use the single-site theory as a tool for learning about physical quantities of large-N QCD with one flavor of adjoint fermions, and large-N QCD with two flavors of fermions in the antisymmetric representation. Reduction allows one to calculate expectation values of Wilson-loops and connected correlation functions of certain fermionic operators, and thus to determine the string-tension and certain ''hadron'' masses, as well as glueball-$\bar{q}q$ mixing, etc. From a practical point of view, however, the key question is this: What value of N is needed to obtain results with controlled $1/N$ corrections? We have made a first step at answering this question by looking at two variables—the average plaquette and the eigenvalue densities of a fundamental-representation massless fermion. The former is not itself a physical quantity, as it is dominated by ultraviolet fluctuations, but it is simple to calculate and can give an indication of the $1/N$ behavior. While our calculations using $N = 8$–15 cannot pin

down the form of the $1/N$ dependence, it does appear that the results at $N = 15$ lie within a few percent of those at $N = \infty$.

The eigenvalue densities provide a test of whether the single-site gauge configurations can reproduce the long-distance physics of chiral-symmetry breaking. In particular, in their ''epsilon-regime,'' the low lying eigenvalues of the Dirac operator have correlated distributions that are predicted by RMT. We find distributions which differ significantly from the RMT predictions, and, based on the results of Ref. [45], take this as evidence that our values of N are too small to probe the epsilon regime.

It is important to stress that, although we find that $N = 8$–15 are too small for this particular observable, these values of N do appear to be sufficient to study the nature of the phase diagram, which is the main goal of this paper.

Looking forward, the prospects for using reduction as a quantitative numerical tool clearly depend on developing or implementing algorithms with a less formidable N dependence than the N^8 scaling of our method. This will allow us to simulate much larger values of N, and see if the phase diagram presented in this paper for $N \leq 15$ is indeed indicative of its $N = \infty$ limit. We are considering implementing a hybrid Monte-Carlo. It also is clear that to move forward one needs greater computing resources. In that regard, one issue to be faced is the lack of any obvious way of parallelizing the code. Here the advantage of reduction—packing as much information as possible into the link matrices—leads to a computational problem.

A less ambitious direction of further study is to make more extensive and systematic measurements of observables on the lattices we already have at hand. We have in mind, in particular, studying the correlators of hadrons composed of adjoint-representation fermions. This would allow us to check our hypothesis that the critical line corresponds to the minimal mass of the pions. We would also like to measure the eigenvalue densities for adjoint-representation fermions. These are expected to enter their epsilon regime for values of N that are parametrically smaller than those required in the fundamental fermions case.

Finally, we recall that using reduction is also of interest for other values of the number of Dirac flavors. In particular, for $N_f = 1/2$, the chiral limit of the theory is related to the $\mathcal{N} = 1$ SUSY gauge theory, while, for $N_f = 2$, the theory is perhaps conformal. If reduction holds for these cases as well, then it provides a method to study the large-N limits of these theories.

ACKNOWLEDGMENTS

We thank H. Neuberger for bringing Ref. [3] to our attention, and Joyce Myers for discussions. This study was supported in part by the U.S. Department of Energy under Grant No. DE-FG02-96ER40956.

[1] M. Teper, Proc. Sci., LATTICE2008 (2008) 022.
[2] T. Eguchi and H. Kawai, Phys. Rev. Lett. **48**, 1063 (1982).
[3] H. Neuberger, Ann. Inst. Henri Poincaré, A **4**, S147 (2003).
[4] P. Kovtun, M. Unsal, and L. G. Yaffe, J. High Energy Phys. 07 (2005) 008.
[5] A. Armoni, M. Shifman, and G. Veneziano, Phys. Rev. Lett. **91**, 191601 (2003); Nucl. Phys. **B667**, 170 (2003); Phys. Rev. D **71**, 045015 (2005).
[6] P. Kovtun, M. Unsal, and L. G. Yaffe, J. High Energy Phys. 06 (2007) 019.
[7] M. Unsal and L. G. Yaffe, Phys. Rev. D **74**, 105019 (2006).
[8] G. Bhanot, U. M. Heller, and H. Neuberger, Phys. Lett. B **113**, 47 (1982).
[9] V. A. Kazakov and A. A. Migdal, Phys. Lett. B **116**, 423 (1982).
[10] M. Okawa, Phys. Rev. Lett. **49**, 353 (1982).
[11] P. N. Meisinger and M. C. Ogilvie, Phys. Rev. D **65**, 056013 (2002); J. C. Myers and M. C. Ogilvie, J. High Energy Phys. 07 (2009) 095; T. J. Hollowood and J. C. Myers, arXiv:0907.3665.
[12] M. Unsal and L. G. Yaffe, Phys. Rev. D **78**, 065035 (2008).
[13] J. C. Myers and M. C. Ogilvie, Phys. Rev. D **77**, 125030 (2008).
[14] B. Bringoltz, J. High Energy Phys. 06 (2009) 091.
[15] P. F. Bedaque, M. I. Buchoff, A. Cherman, and R. P. Springer, arXiv:0904.0277.
[16] J. Ambjorn, K. N. Anagnostopoulos, W. Bietenholz, T. Hotta, and J. Nishimura, J. High Energy Phys. 07 (2000) 013.
[17] M. Hanada, L. Mannelli, and Y. Matsuo, arXiv:0905.2995.
[18] J. Kiskis, R. Narayanan, and H. Neuberger, Phys. Rev. D **66**, 025019 (2002).
[19] A. Gonzalez-Arroyo, R. Narayanan, and H. Neuberger, Phys. Lett. B **631**, 133 (2005).
[20] A. Gonzalez-Arroyo and M. Okawa, Phys. Lett. B **120**, 174 (1983).
[21] W. Bietenholz, J. Nishimura, Y. Susaki, and J. Volkholz, J. High Energy Phys. 10 (2006) 042.
[22] M. Teper and H. Vairinhos, Phys. Lett. B **652**, 359 (2007).
[23] T. Azeyanagi, M. Hanada, T. Hirata, and T. Ishikawa, J. High Energy Phys. 01 (2008) 025.
[24] B. Bringoltz and S. R. Sharpe, Phys. Rev. D **78**, 034507 (2008).
[25] J. Giedt, R. Brower, S. Catterall, G. T. Fleming, and P. Vranas, Phys. Rev. D **79**, 025015 (2009).
[26] M. G. Endres, Phys. Rev. D **79**, 094503 (2009).
[27] J. Giedt, arXiv:0903.2443.
[28] L. Del Debbio, A. Patella, and C. Pica, arXiv:0805.2058; A. J. Hietanen, K. Rummukainen, and K. Tuominen,

arXiv:0904.0864; G. Cossu and M. D'Elia, J. High Energy Phys. 07 (2009) 048.
[29] S. Catterall, J. Giedt, F. Sannino, and J. Schneible, J. High Energy Phys. 11 (2008) 009.
[30] M. E. Peskin, Nucl. Phys. **B175**, 197 (1980).
[31] H. Leutwyler and A. V. Smilga, Phys. Rev. D **46**, 5607 (1992).
[32] J. B. Kogut, J. Polonyi, H. W. Wyld, and D. K. Sinclair, Phys. Rev. Lett. **54**, 1980 (1985).
[33] F. Karsch and M. Lutgemeier, Nucl. Phys. **B550**, 449 (1999).
[34] I. Montvay, Int. J. Mod. Phys. A **17**, 2377 (2002).
[35] K. Demmouche, F. Farchioni, A. Ferling, G. Munster, J. Wuilloud, I. Montvay, and E. E. Scholz, arXiv:0810.0144.
[36] S. R. Sharpe and R. L. Singleton, Jr., Phys. Rev. D **58**, 074501 (1998).
[37] L. Del Debbio, M. T. Frandsen, H. Panagopoulos, and F. Sannino, J. High Energy Phys. 06 (2008) 007.
[38] S. Aoki, Phys. Rev. D **30**, 2653 (1984).
[39] S. Aoki, Phys. Rev. D **33**, 2399 (1986).
[40] M. Teper (private communication).
[41] M. Campostrini, Nucl. Phys. B, Proc. Suppl. **73**, 724 (1999).
[42] J. Kiskis, R. Narayanan, and H. Neuberger, Phys. Lett. B **574**, 65 (2003).
[43] N. Cabibbo and E. Marinari, Phys. Lett. **119B**, 387 (1982).
[44] M. Teper and H. Vairinhos (private communications).
[45] R. Narayanan and H. Neuberger, Nucl. Phys. **B696**, 107 (2004).
[46] B. Bringoltz and L. G. Yaffe (work in progress).
[47] J. C. Osborn, D. Toublan, and J. J. M. Verbaarschot, Nucl. Phys. **B540**, 317 (1999); P. H. Damgaard, J. C. Osborn, D. Toublan, and J. J. M. Verbaarschot, Nucl. Phys. **B547**, 305 (1999).
[48] L. Giusti and M. Luscher, J. High Energy Phys. 03 (2009) 013.